# Late summer early fall phytoplankton biomass (chlorophyll *a*) in the eastern Bering Sea: spatial and temporal variations and factors affecting chlorophyll *a* concentrations

**Lisa B. Eisner[a*], Jeanette C. Gann[b], Carol Ladd[c], Kristin Cieciel[b], Calvin W. Mordy[c,d]**

[a]NOAA-Fisheries, Alaska Fisheries Science Center, 7600 Sand Point Way NE, Seattle, WA 98115, USA, Lisa.Eisner@NOAA.gov, 001-206-526-4060

[b]NOAA-Fisheries, Alaska Fisheries Science Center, 17109 Point Lena Loop Road, Juneau, AK 99801, USA, Jeanette.Gann@NOAA.gov; Kristin.Cieciel@NOAA.gov

[c]NOAA-Pacific Marine Environmental Laboratory, 7600 Sand Point Way NE, Seattle, WA 98115, USA, Carol.Ladd@NOAA.gov; Calvin.W.Mordy@NOAA.gov

[d]Joint Institute for the Study of the Atmosphere and Ocean, University of Washington, 3737 Brooklyn Ave NE, Box 355672, Seattle, WA 98105-5672 USA

*Corresponding Author

## Abstract

The spatial and temporal variability of late summer/early fall phytoplankton biomass estimated from in situ chlorophyll *a* (Chl*a*) concentrations was investigated over a 10-year time period from 2003-2012 in the eastern Bering Sea, encompassing both warm, (2003-2005) and cold (2007-2012) temperature regimes. Warm temperature regimes were characterized by above average water temperatures and low seasonal sea ice extent and cold by below average temperatures and high seasonal sea ice extent. The highest phytoplankton Chl*a* was observed near the Pribilof Islands and the southeastern shelf break where nutrient concentrations were high due to onshore flow from Pribilof and Bering Canyons. The lowest Chl*a* was observed on the northeastern middle and inner shelf, north of Nunivak and St. Matthew Islands and south of St. Lawrence Island (~61- 63°N). Stations north of St Matthew Island (61°N) did not show significant variations in Chl*a* between temperature regimes. To the south, total phytoplankton Chl*a* was significantly higher in warm compared to cold years on the south-outer shelf and on portions of the middle shelf. Large phytoplankton Chl*a* was higher in warm years over most of the southern middle-shelf. For the entire southeastern Bering Sea shelf (~30-200 m bathymetry, south of Nunivak Island), the highest Chl*a* was seen in 2005 and lowest in 2007 and 2008.

On the south-middle shelf, wind mixing and temperature below the pycnocline had strong positive associations with Chl*a* (total and large-size fraction) integrated over the top 50 m, explaining 85% of the variability in mean Chl*a*. This indicates that Chl*a* in summer and early fall is positively affected by wind-induced upwelling of nutrients to the surface and possibly by other bottom up effects such as temperature-mediated growth. Higher bottom temperature is related to reductions in sea ice extent which may elicit ecosystem responses such as reduced biomass of large crustacean zooplankton grazers, potentially due to the removal of ice algae, an important food resource for zooplankton in early spring. This, in turn, could reduce or alter the grazing pressure on phytoplankton later in the growing season. Overall, spatial and temporal variations in phytoplankton Chl*a* are due to a combination of factors, from local inputs of nutrients related to mixing or advection, up to large scale ecosystem effects.

**Keywords: phytoplankton, nutrients, cold pool, chlorophyll *a*, climate, eastern Bering Sea**

## 1. Introduction

Phytoplankton biomass variations (using chlorophyll *a* [Chl*a*] as a proxy) may reflect changes in energy (primary production) available to zooplankton and higher trophic level consumers such as marine birds and fish on the eastern Bering Sea shelf (Brown et al., 2011). Production that is not grazed will sink and support benthic production, often producing benthic "hot spots", particularly in regions with high levels of primary production and large-size, quickly sinking phytoplankton taxa (Grebmeier et al., 2006). Large phytoplankton taxa such as diatoms can also allow for a shorter food web with more efficient energy transfer to higher trophic levels (e.g. diatoms to large copepods such as *Neocalanus* spp. to seabirds, Springer et al., 1996). Phytoplankton metrics (biomass, taxonomy and production) vary spatially across the eastern Bering Sea shelf (Rho and Whitledge, 2007; Brown et al., 2011; Liu et al., this issue) and temporally, both seasonally (Lomas et al., 2012; Moran et al., 2012) and interannually (Brown and Arrigo, 2013).

Spatial variations in phytoplankton metrics may be associated with strong cross-shelf variations in physics and nutrients during summer. This wide (> 500 km) coastal shelf is characterized by a well-mixed inner shelf, a highly stable two-layer water column on the middle shelf, and a three-layer system with a well-mixed surface and bottom layer on the outer shelf (Coachman, 1986). Zooplankton communities (meso- and micro-zooplankton) also show strong cross-shelf gradients (Eisner et al., 2014; Stoecker et al., 2014a, 2014b). Therefore, both bottom-up (e.g. stratification, nutrient concentrations) and top-down factors (e.g. meso- and micro-zooplankton grazing) can produce cross-shelf variations in phytoplankton Chl*a* and size structure. Likewise, variations in phytoplankton production may influence zooplankton abundances. There are also large ecosystem variations within the cross-shelf domains (inner, middle and outer shelf), so it is useful to examine finer scale variation using the smaller spatial areas (regions) defined for the Bering Sea Project (Bering Sea Ecosystem Study [BEST] and Bering Sea Integrated Ecosystem Research Program [BSIERP], Ortiz et al., 2012; Wiese et al., 2012). These regions are based on oceanographic, ecosystem, and fisheries characteristics and parse the eastern shelf into seven regions south and six regions north of ~60 °N (Fig 1).

Interannual variations in phytoplankton metrics may be driven by physical forcing associated with large-scale changes in sea ice extent and water temperature. Marked multiannual shifts in sea ice have occurred during recent years in the eastern Bering Sea, with a series of warm years

with low sea ice extent (warm temperature regime, 2000-2005) followed by a series of cold years with extensive sea ice (cold temperature regime, 2007-2013) (Stabeno et al., 2012b; Zador, 2014). However, it is debated whether warming will increase or decrease biological productivity (Brown et al., 2011; Lomas et al., 2012; Brown and Arrigo, 2013; Liu et al., this issue), partially due to uncertainty of how temperature regime changes will affect nutrient availability. Phytoplankton biomass, production, size structure and taxonomic composition have been evaluated for recent cold years (2008-2010); but few studies were conducted during recent (early 2000s) warm years (Strom and Frederickson, 2008; Liu et al., this issue), so data are limited for temperature regime comparisons.

The timing of primary production is important to functioning of the Bering Sea ecosystem (Sigler et al., this issue). Many prior studies on the eastern Bering Sea shelf have focused on production and biomass during spring (when the bulk of the yearly production is thought to occur) and early summer periods on the eastern Bering Sea shelf (McRoy et al., 1972; Sambrotto and Goering, 1983; Sambrotto et al., 1984, 1986, 2008; Walsh and McRoy, 1986; Whitledge et al., 1986; Hansell et al., 1993; Springer et al., 1996; Kopylov et al., 2002; Rho and Whitledge, 2007; Lomas et al., 2012). However, fewer studies have focused on understanding variations in phytoplankton ecology during late summer and early fall, near the end of the growing season (Springer and McRoy, 1993; Rho and Whitledge, 2007; Strom and Frederickson, 2008; Sigler et al., 2014; Liu et al., this issue) and none of those studies covered a large number of consecutive years for the entire eastern Bering Sea shelf. Summer and early fall are critical periods for growth of many larval and juvenile fish in the eastern Bering Sea (Duffy-Anderson et al., 2006; Sigler et al., this issue), and this is an important time for lipid accumulation in age-0 Walleye Pollock (*Gadus chalcogrammus*) and other forage fish prior to overwintering (Siddon et al., 2013; Sigler et al., this issue).

The goal of this manuscript is to synthesize ten years of phytoplankton Chl*a* data and associated physical and chemical variables (hydrography, nutrients, and wind mixing) collected during late summer/early fall across the entire eastern Bering Sea shelf. Variations in total and large-size phytoplankton Chl*a* will be described both spatially (north-south and cross-shelf) and interannually over extended temperature regimes. We describe spatial variability over the entire shelf, and for the southern middle shelf domain we investigate interannual variability and

environmental factors related to these variations (temperature, salinity, August stratification, summer wind mixing and nutrients). We chose to focus on this domain (50-100 m bathymetry, south of ~60°N) since it has a long record of environmental variability (e.g., sea ice, temperature, salinity) from mooring observations collected by the Pacific Marine Environmental Laboratory (PMEL). During summer, the southern middle shelf domain has warm surface temperatures and cool bottom temperatures separated by a sharp pycnocline (Coachman, 1986). A cold pool (bottom temperatures < 2 °C) expands southward into the southern middle shelf only during years with high southerly sea ice extent, so there is high variability between temperature regimes. Large variations in zooplankton community composition have also been observed on the south-middle shelf between temperature regimes (Eisner et al., 2014), resulting in changes in prey availability for key forage fish in this area, such as age-0 Walleye Pollock and Pacific Cod (*Gadus macrocephalus*) (Heintz et al., 2013). For our environmental factor analysis, we focus on two sub-regions of the south-middle domain that encompass two long-term oceanographic moorings, PMEL Mooring 2 (M2, Region 3) and Mooring 4 (M4, inshore of the Pribilof Islands, Region 6) (Fig. 1). We also evaluate the timing and strength of the fall blooms from ocean color Chl*a* measurements for the entire southeastern middle shelf (Regions 1, 3, 5 and 6).

## 2. Data and Methods

### *2.1 Temperature regime designation*

Years used in this analysis were designated as warm (2003-2005), average (2006) or cold (2007-2012) based on depth-averaged temperature anomalies on the southeastern middle shelf (Stabeno et al. 2012b, Zador, 2014). Water temperatures reflect southerly ice extent and timing of retreat, with colder temperatures associated with increased southerly ice extent and later retreat compared to years with warmer temperatures. Water temperature between temperature regimes varied by an average of ~3°C for both surface and deep waters on the south-middle shelf in late summer (Eisner et al., 2014).

### *2.2 Phytoplankton Chla biomass and size structure, hydrography and nutrients*

From 2003-2012, Bering-Arctic Subarctic Integrated Survey (BASIS) hydrographic data were collected at stations spaced ~60 km apart, over a survey grid which spanned the shelf (160-172°W, 54.5-65 °N, Fig. 1). Sampling occurred from mid-August to early October, although survey start and end times varied by up to three weeks among years (Table 1). Conductivity-temperature-depth (CTD) measurements were collected with a Sea-bird (SBE) 911 or SBE 25 CTD equipped with a Wetlabs Wet-Star or ECO fluorometer. Water samples for nutrients and total and size-fractionated Chl*a* were collected during the upcast with Niskin bottles attached to the CTD. Nutrient samples were collected at 2 to 6 depths distributed above and below the pycnocline. Samples were frozen at -80 °C on board ship and analyzed for dissolved phosphate, silicic acid, nitrate, nitrite, and ammonium at a shore-based facility using colorometric methods (JGOFS, 1994). Dissolved inorganic nitrogen (DIN) was estimated by summing nitrate, nitrite, and ammonium.

It has been shown that freezing may be problematic to ammonium measurements (Grasshoff, 1976; ICES, 2004). To evaluate this potential error in our data set, we compared samples collected in similar locations (within 60 km) and depths within a two-week period on two different cruises on the eastern Bering Sea shelf in 2005 (Mordy et al., 2010). On one cruise samples were stored frozen while on the second cruise samples were analyzed at sea. Analytical methods were the same for both sample sets (modified indophenol blue method; Slawyk and MacIsaac, 1972; Mantoura and Woodward, 1983). Ammonium sample concentrations in 2005 ranged from 0.1 to ~ 10.5 μM (after removal of one outlier of 12.3 μM), similar to our entire data-set. This analysis indicated a strong linear relationship between frozen and unfrozen ammonium samples ($N$= 61, $R^2$ = 0.89, $P$ < 0.001), although values were slightly (17% on average) higher for frozen samples (paired t-test, $P$ = 0.004, 95% CI for differences = 0.14 to 0.73, mean = 0.44). Some of the difference between unfrozen and frozen samples was likely due to variations in collection dates and locations. Based on this evaluation, we chose to include ammonium values from frozen samples in our analysis.

Chl*a* samples were collected at similar depths as nutrients. Samples were filtered through Whatman GF/F filters (nominal pore size 0.7 μm) to estimate total Chl*a*, and through polycarbonate filters (pore size 10 μm) to estimate large-size fraction Chl*a*. Filters were stored frozen (-80°C) and analyzed within 6 months with a Turner Designs (TD-700) bench top

fluorometer following standard methods (Parsons et al., 1984). In vivo fluorescence data, calibrated with discrete Chl*a* samples by fluorometer and year (mean $R^2$ = 0.68 (standard deviation (sd) 0.13), mean N = 250 (sd 140)) were used to calculate integrated Chl*a* over the top 50 m, or to the bottom for station depths less than 50 m. The integrated >10 µm (large) size-fractionated Chl*a* was similarly estimated by multiplying the total integrated Chl*a* from calibrated in vivo fluorescence data by the mean large-size fraction ratio (>10 µm Chl*a* /total Chl*a*) from discrete samples. The integrated <10 µm (small) size-fractionated Chl*a* was estimated by subtraction of the large-size fraction from the total integrated Chl*a*. We used in vivo Chl*a* data for our integrations since discrete Chl*a* samples (total and size-fractionated) did not provide sufficient vertical resolution (ranged 10-30 m between sample depths).

Station locations sampled 5 years or more were used for all graphical and statistical analysis (Fig. 1) for a total of ~1000 sampling events for all years combined. This 5-year cutoff eliminated stations sampled only a few times (near the edge of our grid or with uneven station spacing). The following means were determined for each region and each year: integrated total and large-size fraction Chl*a*, and T, S and nutrients in surface and deep waters. For T and S, we used mean values above and below the pycnocline, since these were most representative of surface and deep water masses. The depth of the pycnocline (mixed layer depth) was defined as the first depth where sigma-t was 0.10 kg $m^{-3}$ higher than the 5 m value (Danielson et al., 2011). Since nutrient data were sparser than for T and S, 5 m nutrient samples were considered representative of the surface layer and 30-60 m samples representative of the deep layer. Preliminary plots indicated that relative spatial patterns of Chl*a* and nutrients were fairly consistent among years; therefore, we used data from all years combined to visualize the average late summer spatial distributions. ArcMap (ESRI, 2014) with Natural Neighbor contouring was used to make horizontal contour maps of integrated Chl*a* (total and large-size fraction), surface and deep nitrate, ammonium, DIN, and silicic acid. Integrated Chl*a* and surface and deep temperatures were also plotted separately for warm years and cold years.

To statistically evaluate differences in Chl*a* between temperature regimes for each region, we used mixed models in SYSTAT (Systat Sofware Inc., 2009) with Residual or Restricted Maximum Likelihood (REML), with station location and year nested within regime as random effects. Analyses were conducted on mean natural log transformed integrated Chl*a* (total, large

and small size fractions), surface and deep T and S, transformed ($4^{th}$ root transformation) surface and untransformed deep DIN and silicic acid, for warm and cold years for each Bering Project Region (1-14, excluding 8). Region 8 was excluded due to small sample size (infrequent sampling). To visualize interannual variations in Chl*a* among regions, we computed standardized anomalies (standardized to maximum anomaly value) for natural log transformed integrated Chl*a* (total and large size-fraction) for each year and region.

*2.3 Stratification*

A stratification index using data from the PMEL M2 mooring located on the south-middle shelf (56.9°N, 164.1°W) was determined following the methods described in Ladd and Stabeno (2012). Potential energy relative to the mixed state (J $m^{-2}$) can be used as a stratification index (*SI*):

$$SI = \int_{-h}^{0} (\rho - <\rho>) gz dz; \quad <\rho> = \frac{1}{h}\int_{-h}^{0} \rho dz$$

where $\rho$ is density and *h* the depth of the water column (Simpson et al., 1977). The stratification index is equal to 0 for a vertically mixed system and increases with increasing water column stability. *SI* was integrated to h = 70 m (approximate bottom depth at M2).

For the average August stratification index at M2, we used the data from Ladd and Stabeno (2012) updated with two additional years (2011 and 2012). Similar calculations were also conducted using temperature and salinity measurements from BASIS surveys for 2002-2009 to determine areas of higher and lower stratification. For this analysis, we used data from the top 70 m or bottom, whichever was shallower to estimate the mean (J $m^{-3}$) instead of the integrated (J $m^{-2}$) water column stratification.

*2.4 Wind mixing*

Friction velocity cubed ($u_*^3;\ m^3\ s^{-3}$) is proportional to the rate of mechanical energy applied at the ocean surface for stirring (Bond and Adams, 2002) and was used as a proxy for wind mixing. Data for summer months (June-August) were obtained from National Centers for Environmental Prediction (NCEP) reanalysis data set (Kalnay et al., 1996) and were averaged over 2° latitude by 5° longitude boxes (N. Bond, NOAA PMEL, pers. comm.) centered over each of the NOAA

PMEL moorings, M2 (56.9°N, 164.1°W) and M4 (57. 9°N, 168. 9°W; Stabeno et al., 2010). As wind speeds at M2 and M4 are similar and winds in the southeastern Bering Sea show strong coherence over large spatial areas (Stabeno et al., 2010), we assumed M2 and M4 winds approximated wind fields over the Bering Project Regions 3 and 6, respectively. The number of days that exceeded a threshold $u_*^3$ value of 0.05 $m^3$ $s^{-3}$ (one standard deviation above mean daily $u_*^3$ for June-August for 2000-2012) at M2 was used as an index of the frequency of summer wind mixing events.

*2.5 Timing and strength of the fall bloom from ocean color observations*

Moderate Resolution Imaging Spectroradiometer (MODIS) ocean color data were used to generate monthly (August, September, October) composites of mean Chl*a* (mg $m^{-3}$) over the south-middle shelf for Regions 1, 3, 5, and 6 (Fig. 1). High cloud cover precluded the use of 8-day or bi-weekly composites. For the monthly composites, regions or months with less than 50% data coverage were excluded from the analysis. The months of highest Chl*a* within each region (all years combined) provides a rough estimate of the timing of the fall surface phytoplankton bloom on the south-middle shelf. Summation of the average Chl*a* for August, September and October (termed Aug-Oct MODIS) for Region 3 (area surrounding M2) was used as an index of the magnitude of the fall bloom. In situ Chl*a* data (5 m depth) from discrete samples collected on BASIS surveys were included for comparison.

*2.6 Mechanisms influencing integrated Chla*

Environmental variables potentially related to variations in integrated total and large-size fraction Chl*a* in Regions 3 and 6 during late summer/early fall were evaluated visually, followed by Generalized Linear Models (GLM) using backwards stepwise selection (Type 3 Sum of Squares) in SYSTAT. The environmental variables tested included means for August $u_*^3$ (~2 weeks prior to sampling), August stratification index at M2, in situ surface T, deep T and deep S, and surface and deep nutrients (nitrate, ammonium, and silicic acid), using depths defined above (*Section 2.2*). Surface salinity and surface phosphate were not included in GLM analysis since they were found to be highly correlated with other variables (deep T and surface ammonium, respectively, Pearson correlation > 0.85). Stratification data were not available at M4 for many of the years, so this variable was not included in the model for Region 6. Finally, to determine if

there was a relationship between Chl*a* and relative size structure, we conducted linear regressions between mean integrated total Chl*a* and percent large phytoplankton (>10 µm Chl*a*/ total Chl*a*) for all regions.

## 3. Results

### *3.1 Phytoplankton biomass and size structure, hydrography and nutrients for entire shelf*

#### *3.1.1 Spatial variation*

There was considerable spatial variability over the shelf for all years combined (2003-2012) for integrated Chl*a* (total and large-size fraction), surface and deep nitrate, DIN and silicic acid and stratification over the top 70 m (Table 2, Figs. 2 and 3). The areas with the highest integrated total Chl*a* were the southern-most region of the inner shelf (Region 2), the southern middle shelf north of the Alaska Peninsula (Region 1), near M4 (Region 6) and around the Pribilof Islands (Region 5), over the south-outer shelf (Region 4), north of St. Lawrence Island (Region 12), and at the single shelf break station (Region 16) (Fig 1, 2A). The areas with the lowest integrated Chl*a* were the north-inner and north-middle shelf (Regions 11, 10), Norton Sound (Region 14) and the region surrounding M2 (Region 3). The high integrated Chl*a* on the south-outer shelf was primarily from small phytoplankton (large < 25% of total Chl*a*), while the relatively high biomass near the Pribilof Islands and M4, and on the south-inner shelf was from a mix of large and small assemblages (large ~50-75% of total Chl*a*) (Fig. 2A, B). In general higher concentrations of large cells were seen in regions with higher total integrated Chl*a*.

Spatial patterns in nitrate and DIN reflected the locations of the cross-shelf domains; nitrate and DIN were mostly depleted throughout the water column in the well-mixed inner domain, and nitrogen-replete deep water was overlain by depleted surface water in the 2-layer middle shelf (Fig. 3A, C, E, G). The highest surface nitrate and DIN were found in the south-outer shelf and offshore, and north of St. Lawrence Island, with the remainder of the shelf generally depleted (< 0.5 µM nitrate and < 1 µM DIN, Fig. 3A, C). The highest deep nitrate and DIN was seen over the southern middle and outer shelf, with low values seen in the northern inner and middle shelf (Fig. 3E, G). The deep DIN values were ~ 5 µM higher than nitrate levels in the south-middle

domain due to the presence of a deep ammonium pool (Fig. 3F); these high ammonium concentrations are commonly observed at depth in this domain during summer (Kachel et al., 2002; Mordy et al., 2008). Surface silicic acid concentrations over the entire shelf were generally in the range of 3-7 µM, with the highest concentrations over the southern outer shelf and in Norton Sound (Fig. 3D). Deep silicic acid was higher over most of the southern middle and outer shelves and around St. Lawrence Island, and lower over much of the south-inner shelf (Fig. 3H), similar to nitrate and DIN. The highest stratification was observed in the south-middle shelf in Region 3 (Fig. 4), a region characterized by low Chl*a* and small cells, and elevated ammonium in the deep water.

### *3.1.2 Temporal Variation*

Integrated total and large-size fraction Chl*a* show similar spatial patterns across temperature regimes, but values were higher in warm (2003-2005) than in cold (2007-2012) years for all southern regions and most northern regions (Fig. 5A, B, E, F). Significant differences between temperature regimes for integrated Chl*a* (total, large-size and small-size fraction) were only seen in middle and outer shelf regions at or south of 61° N (near St Matthew Island and south) (Table 3, Fig. 1). In warm years, there was higher total Chl*a* for Regions 1, 4 and 9, and higher large-size fraction Chl*a* for Regions 1, 3, 4, 6 and 9. The small-size integrated Chl*a* was also higher in two of the regions that had higher total integrated Chl*a* (Regions 4 and 9). Similarly, surface and bottom temperature (Fig. 5C, D, G, H) and salinity (not shown) were significantly higher in warm compared to cold years only in regions at or south of 61°N (Table 3). Significant differences in salinity were only observed in the middle domain (Regions 3, 5, 6, and 9), while difference in temperature were seen in all cross-shelf (inner, middle and outer) domains. There were no significant differences for surface or deep DIN or silicic acid between warm and cold regimes ($P > 0.10$).

Interannual variations in Chl*a* were also observed. Total and large-size fraction integrated Chl*a* were high in 2005 (and secondarily in 2004) in most southern regions and near St. Matthew Island (Region 9) and low in 2006 and 2007 (and to some extent 2008) in more disparate regions (Table 2). There were significant linear relationships (ANOVA, $P < 0.05$) between mean integrated Chl*a* and percent large-size fraction for Regions 1, 3, 4 and 10 for 2003-2012 (Fig. 6). The north-middle shelf (Region 10) had a smaller range of variability in percent large Chl*a* than

regions farther south, suggesting phytoplankton size classes were more consistent across years in the north compared to the southeastern Bering Sea shelf.

### *3.2 Stratification, wind mixing and phytoplankton biomass on the southeast middle shelf*

#### *3.2.1 Stratification and wind mixing*

August stratification intensity, August $u_*^3$ (a proxy for wind mixing magnitude), and the number of threshold wind mixing events (> 0.05 $m^3$ $s^{-3}$) for summer (June-August) did not vary significantly between temperature regimes in Region 3 ($P$ = 0.12, $P$ = 0.33, and $P$ = 0.92, respectively, t-test, Table 4). The highest August stratification was seen in 2004 and 2007, and the lowest number of wind mixing events was in summer 2007, indicating that conditions during 2007 were anomalously stable. Low integrated Chl*a* (total and large-size fractions) were observed in 2007 (Table 2). In contrast, August stratification in 2005 was average, while August $u_*^3$, number of summer wind mixing events and integrated total and large-size fraction Chl*a* were the highest in our time series.

#### *3.2.2 Mechanisms influencing phytoplankton biomass*

Linear regressions of single environmental variables in the southeast middle domain show a positive relationship between August $u_*^3$ at moorings M2 and M4 and mean integrated total Chl*a* for Regions 3 and 6 ($R^2$ = 0.77 and 0.69, respectively, $P$ < 0.05 ANOVA, Fig. 7), with the highest wind mixing indicated in 2005. Removal of 2005 data from the analysis yields $R^2$ = 0.43 and 0.23 ($P$ = 0.05 and 0.11) for Regions 3 and 6, respectively. Positive relationships also were seen for deep T and integrated total Chl*a*, with a weaker relationship in Region 3 than in Region 6 ($R^2$ = 0.50 and 0. 83, respectively, $P$ < 0.05 ANOVA, Fig. 7). Similar to wind mixing, removal of 2005 from the analysis reduces the correlation, with $R^2$ = 0.28 and 0.76 ($P$ = 0.15 and 0.002) for Region 3 and 6, respectively. Stepwise multiple linear regressions show that the best model for predicting integrated total Chl*a* for Region 3 includes August $u_*^3$, deep T and August stratification (Table 5). Similarly, the best model for Region 6 included August $u_*^3$ and deep T. August stratification was not included in the regression model for this region as no data were available. These models explain 86-96% of the interannual variation in integrated total Chl*a*, with 85-86% explained by $u_*^3$ and deep T alone. Similar to total Chl*a*, $u_*^3$ was positively related to large-size fraction Chl*a* for both Regions 3 and 6. However, deep T was only significant for

large-size fraction Chl*a* in Region 3 (Table 5). Deep nutrients were important in both Regions 3 and 6, with a negative relationship for silicic acid in Region 3 and a positive relationship for ammonium in Region 6. Similar to total Chl*a*, these factors explained 83-96% of the variability in large-size fraction Chl*a*.

### *3.3 Timing and strength of fall blooms from ocean color data*

Comparisons of monthly averages of Chl*a* from MODIS ocean color measurements for the south-middle regions combined (Regions 1, 3, 5 and 6) indicated that Chl*a* concentrations were lowest in August ($P < 0.05$, ANOVA), with similar Chl*a* during September and October ($P > 0.05$) (Fig. 8A). Among these three months, the highest Chl*a* was in September and October for the majority of the south-middle shelf area (Regions 3 and 6), and in September near the Alaska Peninsula (Region 1) and surrounding the Pribilof Islands (Region 5). Interannual variability in MODIS data is somewhat consistent with in situ 5 m Chl*a* data (higher values in 2005 and 2009 in both datasets), although the high in situ values for 2011 were not observed in the MODIS data (Fig. 8B). Lower values were observed in 2007, 2008 and 2012 in both data sets.

## 4. Discussion

The over-arching goals of this study are to evaluate spatial and temporal variability in phytoplankton Chl*a* during late summer/early fall, associated environmental variables driving this variability and potential ecosystem interactions. We discuss 1) the spatial variability of phytoplankton biomass and associated physical and chemical oceanographic variables, 2) the temporal variations (interannual and between temperature regimes) in phytoplankton Chl*a* over the entire eastern Bering Sea shelf and the environmental factors associated with these variations (for the south-middle shelf, in particular), 3) implications for fisheries, and 4) estimations for fall bloom timing on the south-middle shelf.

### *4.1 Spatial variability*

Phytoplankton Chl*a* showed considerable spatial variations during late summer/early fall likely due to variations in nutrient availability from horizontal advection, e.g. along-shelf currents, flows through canyons (Kinney et al., 2009; Stabeno et al., 2010, this issue) and/or vertical

upwelling/mixing of nutrient-rich waters (Sambrotto and Goering, 1983; Sambrotto et al., 1986; Kachel et al., 2002). Preliminary maps (data not shown) indicate that the relative distribution patterns were also fairly similar among years (e.g. Pribilof Islands and south-outer shelf had relatively high Chl*a*; north of 61°N had relatively low Chl*a*).

*4.1.1 North–South variations*

The low Chl*a* observed on the north-middle shelf between 61-63 °N (Fig. 2) was associated with relatively low nitrate and ammonium below the pycnocline (implying that wind mixing events would be less effective at mixing nutrients to the surface). Since this region had lower stratification than the southern middle shelf (Stabeno et al., 2012a; Fig 3), less energy (lower wind speeds) would be necessary to mix the water column. Thus, deep nutrients may be decreased in this region due to summer wind mixing (prior to our survey time period) or from the prevalence of sub-pycnocline primary production observed in the northern middle shelf (Stabeno et al, 2012a; Mordy et al., 2012). This could lead to greater draw-down of deep nutrients in this region than on the middle shelf farther south. In addition to wind mixing, the canyons that incise the shelf-break can result in on-shelf flux of nutrients. Stabeno et al. (this issue) estimate that over 50% of nutrients are replenished on the southern middle shelf each year with much of that coming from the deep basin through the Bering Canyon (Fig. 1), which may explain the high levels of deep nutrients near the shelf-break and intruding into the middle shelf in the south. Slope water does not appear to greatly replenish the inner shelf (Granger et al., 2012). Unfortunately, we did not collect data on the northern shelf at bathymetry > 70 m, so we cannot evaluate variations on the northern outer shelf or shelf-break.

Phytoplankton Chl*a* (both total and large-size fraction) did not vary significantly between temperature regimes in regions north of 61°N, unlike several southern regions; this coincides with lower variability in surface and deep T and S in the north compared to the south (Fig. 5; Stabeno et al., 2012a). Likewise, variability in zooplankton community composition between temperature regimes was lower in the northeastern compared to the southeastern Bering Sea shelf during late summer/early fall (Eisner et al., 2014). The northern Bering Sea is always seasonally ice covered (Stabeno et al., 2012a, with some exceptions influenced by polynyas) with more consistent ice coverage, timing of ice retreat and timing of the spring bloom compared to the southern Bering Sea (Sigler et al., 2014). Both ice algae and ice edge spring blooms occur

annually in this northern region unlike the southern shelf which only has ice associated production in cold years. Thus, an early spring food source (phytoplankton or ice algae) for large crustacean zooplankton may be available in both warm and cold years on the northern shelf, although there are still variations among regions within the northern shelf. In general, we may expect lower trophic pelagic organisms (ice algae, phytoplankton and zooplankton) to be less affected by temperature regime changes in the northern compared to the southeastern Bering Sea.

Benthic biomass also varies between the north and south Bering Sea shelf with a predominance of invertebrates in the north (McCormick-Ray et al., 2011). Benthic biomass is fueled by sinking organic material, so areas of higher benthic biomass may coincide with areas with high abundances of larger faster sinking phytoplankton or ice algae (e.g. large diatoms). Grebmeier et al. (2006) described patterns of integrated Chl*a* in the northern Bering Sea for April to September 1976-2004, and found that concentrations were lower from 60 to 62 °N (Region 9), Norton Sound (Region 14) and the north-inner shelf (Region 11), and higher north of St. Lawrence Island (Regions 12 and 13). These patterns are generally similar to the current study, although for the area south of St. Lawrence Island (Region 10), higher values were observed by Grebmeier et al. (2006). A majority of the primary production in the northern Bering Sea reaches the benthos likely due to short food chains and shallow bathymetry (Grebmeier et al., 2006), high sub-pycnocline production (Mordy et al., 2012; Stabeno et al., 2012a), a high annual flux of ice algal production, and temperature restriction of grazing pressure. This sinking production fuels large benthic invertebrate communities (epifauna and infauna) in areas that coincide with water column production hot spots (Grebmeier et al., 2006). For example, epifaunal biomass was higher north of St. Lawrence Island, and northeast of St. Mathew Island, and lower from ~61 to 63 °N, east of ~172 °W; this corresponds with higher and lower integrated Chl*a* seen in our current study. Epifaunal biomass was also relatively high west of 172 °W, outside our study area, in an area where high Chl*a* was observed along the 70 m isobath (Stabeno et al., 2012a).

#### 4.1.2 Cross-shelf and finer scale variations

Phytoplankton Chl*a* and taxonomic composition varied offshore to onshore and at finer scales as observed in prior studies (e.g. Goering and Iverson, 1981; Brown et al., 2011; Lomas et al., 2012; Moran et al., 2012;). Similarly, primary production has been shown to decrease from offshore to onshore on the southern shelf (e.g., Hansell et al., 1993; Springer et al., 1996; Lomas

et al., 2012). High Chl*a* along the shelf break, as observed for our single shelf-break station (Fig. 1), is a well-established phenomenon due to high nutrient availability from mixing of oceanic waters at this front (e.g. “green belt”, Springer et al., 1996). In the south-outer domain (Region 4) the higher Chl*a* was associated with higher surface nutrient concentrations (nitrate and silicic acid, Fig. 2A, D) due to on-shelf flow through Bering Canyon (Stabeno et al., this issue). Likewise, the higher percentage of small cells observed in this region were likely of oceanic origin, transported by on-shelf flows. Due to the break-down of the frontal structure in fall, cross-shelf fluxes are higher in fall than summer (Stabeno et al., this issue).

In the south-middle domain, finer scale variations in phytoplankton Chl*a* and size structure were observed among the four regions (Regions 1, 3, 5, 6). The somewhat higher Chl*a* (total and large-size fraction) near M4 (Region 6) compared to M2 (Region 3) may be due in part to the relatively lower stratification at M4 (Fig. 4; Ladd and Stabeno, 2012), which may allow a greater flux of nutrients to the surface during wind events. Nitrogen was usually the limiting nutrient on the south-middle shelf, with the exception of 2007 when silicic acid was likely limiting to diatom growth in Region 3 (Gann et al., this issue). The region north of the Alaska Peninsula (Region 1) is influenced by the Alaska Coastal Current (ACC). The ACC flows through the eastern Aleutian Passes and mixes with nutrient-rich slope waters before flowing on-shelf toward the east along the Alaska Peninsula; this flow provides a relatively constant supply of nutrients (Stabeno et al., 2002) which may fuel production there throughout the summer. Near the Pribilof Islands (Region 5), the high Chl*a* and relatively high surface nitrate, ammonium and silicic acid is due to the influx of nutrients along the 100-m isobath with intrusions from Pribilof Canyon, and the westward transport and vertical mixing of middle-shelf water containing nutrient-rich (high ammonium and nitrate) bottom water (Stabeno et al., 2008, this issue; Sullivan et al., 2008). Prior studies have found the tidally mixed region adjacent to the Pribilof Islands to have high primary production throughout the summer (Sambrotto et al., 2008) which contributes to the high abundance of planktivorous and piscivorous seabirds (e.g., murres, kittiwakes, puffins, auklets and others) and pinnipeds (e.g., northern fur seals) (Byrd et al., 2008; Call et al., 2008; Hunt et al., 2008; Jahncke et al., 2008). Our study confirms that the Pribilof region has the highest phytoplankton Chl*a* on the shelf in both warm and cold years.

In the south-inner domain (Regions 2 and 7), the moderate large-fraction Chl*a* may have been fueled by nutrient inputs at the inner front (Kachel et al., 2002). Nutrient uptake was likely immediate since ambient DIN concentrations were low (< 1 μM, Fig. 2C). Interestingly, surface ammonium was observed in higher concentrations than nitrate (Fig. 2A, B). Recent taxonomic analysis for 2012 indicated that many of the diatoms observed in this region were degraded and lacking chloroplasts, with few long intact chains (data not shown), possibly due in part to large senescent cells being mixed up from the bottom and suspended in the water column by tidal mixing. However, some fraction of the phytoplankton biomass was actively growing; surface primary production rates in the inner domain, estimated at a subset stations in the current study, were moderate (Liu et al., this issue). Other studies have also found appreciable production in the inner domain regions during summer (Rho and Whitledge, 2007; Brown et al., 2011).

North of St. Lawrence Island (Regions 12 and 13), the high Chl*a* in both warm and cold years is due to high nutrients in the Anadyr Current which continuously fuel production near the surface (Sambrotto et al., 1984; Springer and McRoy, 1993; Grebemeier et al. 2006). This water is advected from the Gulf of Anadyr and flows northeastward through Anadyr Strait into Bering Strait and the Chukchi Sea (e.g., Coachman et al. 1975; Walsh et al., 1989).

*4.2 Temporal variability*

Warm years generally had higher mean late summer/early fall Chl*a* than cold years. Chl*a* and primary production are positively related on an annual basis for the eastern Bering Sea shelf ($R^2$= 0.65, Brown et al., 2011), so higher Chl*a* is likely to be associated with higher productivity. Recent analysis of satellite MODIS data for summer (defined as July-September in their study) attributed higher primary production in warm years to presumed weaker stratification and increased mixing of nutrients to the surface (Brown and Arrigo, 2013). However, there were no significant differences in stratification in warm and cold years for the southeast middle shelf based on M2 data for our survey years (2003-2012) or found by Ladd and Stabeno (2012) for 1995-2010. Other studies suggest that annual production may be lower (Lomas et al., 2012) or similar (Liu et al., this issue) in warm compared to cold years. Modeled annual gross phytoplankton production in the north was found to be higher in warm than cold years, due to the persistence of sea ice in cold years in spring, but was similar between regimes for the south in spring and for the entire shelf in summer (Liu et al., this issue). The high spatial and interannual

variability make it difficult to resolve this issue; it has been estimated that changes would have to exceed a factor of two to be detected (Lomas et al., 2012).

Variations in nutrient concentrations at depth could impact biomass and production, since the flux to the surface will vary for a given magnitude of wind mixing. Deep ammonium was found to be positively related to large-size fraction Chl*a* near M4 (Region 6) using general linear models (Table 5). Salinity below the pycnocline was ~ 0.5 units higher in warm years in this region (Appendix). Cold, northerly winds result in westward (directed off-shelf) Ekman transport and thus, cold summers with higher freshwater content (Danielson et al., 2011, 2012). Warm years exhibit higher on-shelf fluxes of salty, nutrient-rich water (Stabeno et al., 2001). Salinity and nutrients have been shown to be positively related in the eastern Bering Sea (Mordy et al., 2005), suggesting that deep nutrient concentrations are higher in warm years. In our study we could not detect differences between regimes for DIN collected between 30-60 m, possibly due to the non-conservative nature of nutrients closer to the surface. Comparisons of near-bottom nutrients may offer more insight but unfortunately, bottom nutrients were not consistently sampled during all years of our surveys.

Wind mixing (two weeks prior to sample collection) and in situ bottom temperature were the most important factors related to changes in Chl*a*. The positive association with wind mixing following a two week lag time is expected, since time is required for the water column to stabilize after a storm event (so that adequate light is available) and for phytoplankton to grow. Increased primary production has been observed following wind mixing events for several studies on the southeast Bering Sea shelf (e.g., Sambrotto et al., 1986; Mordy et al., 2012).

The positive relationship between bottom temperature and Chl*a* could be related to bottom-up effects such as temperature effects on growth rates (Eppley, 1972), top-down effects such as a reduction in grazing pressure on phytoplankton (Goering and Iverson, 1981), or a combination of these factors. Both bottom and surface temperatures were higher in warm years, so temperature-mediated growth could increase biomass throughout the water column in warm years. However, the temperature response of normalized productivity (mg C mg Chl$a^{-1}$ $h^{-1}$) for 2008 and 2009 indicated that above a threshold of ~5°C, productivity decreased (Lomas et al., 2012). In our study, temperatures in the surface mixed layer were above this threshold for all regions in both

warm and cold years with the exception of the region near St. Matthew Island in 2012 (Appendix).

Bottom temperature during late summer/early fall may be indirectly related to grazing pressure on phytoplankton. Bottom temperature largely reflects the location of the cold pool, which extends farther south in cold years when ice coverage is farther south (Stabeno et al., 2012b). The presence of sea ice in late winter and spring affects the availability (timing and magnitude) of ice algae and phytoplankton prey for zooplankton and larval fish, and thus impacts the ecosystem at many trophic levels. An early algal food source may enhance reproduction in spring of large copepods such as *Calanus* spp. and other-ice associated taxa (Baier and Napp, 2003). Cooler temperatures can also reduce respiration costs throughout the year, and reduce the presence of zooplankton grazers over the middle shelf (Coyle et al., 2008, 2011; Sigler et al., 2014). These favorable conditions in cold years can lead to high zooplankton biomass throughout the growing season. Accordingly, large crustacean zooplankton such as *Calanus* spp. and euphausiids had higher abundances in cold compared to warm years during summer and early fall for our current study years (2003-2010) (Coyle et al., 2011; Ressler et al., 2012; Eisner et al., 2014). The higher Chl*a* and greater percentage of large-size phytoplankton seen in late summer in warm compared to cold years may be partially related to a reduction in large zooplankton abundance and subsequent reduction in grazing pressure, on large phytoplankton, in particular (Goering and Iverson, 1981). This hypothesis suggests that the lower trophic level community structure and biomass observed late in the growing season (August–October) may be set, at least partially, during spring. However, to confound this issue, new research has shown that microzooplankton are the primary grazers of phytoplankton in summer (Stoecker et al., 2014a), so the effects of grazing on phytoplankton biomass may be more complicated. It is unknown if microzooplankton are in higher abundance or have increased grazing rates in warm compared to cold years on the eastern Bering Sea shelf. Although microzooplankton grazing was found to be lower in a single, highly stratified, warm year (2004) than in cold years (2008-2010) (Olson and Strom, 2002; Strom and Frederickson, 2008; Stoecker et al., 2014a; Liu et al., this issue), there are not sufficient data sets to determine conclusively if microzooplankton are in higher abundance or if they have increased grazing rates in warm compared to cold years.

Over the shelf, the average percent large biomass (> 10 µm Chl*a*/total Chl*a*) was 42% in warm years and 30% in cold years (similar to cold year results for June-July 2008 and 2009 for > 5 µm size fractions, Lomas et al., 2012). Phytoplankton biomass in summer 2008 was dominated by flagellates (dinoflagellates and microflagellates) with diatoms in high concentrations at a few locations (e.g., near the Pribilof Islands) (Moran et al., 2012). Therefore, the larger phytoplankton in our study may be a combination of diatoms and dinoflagellates. The transfer of energy up the food web may be more efficient with large phytoplankton (e.g., large phytoplankton to large zooplankton to fish) than occurs with small phytoplankton taxa, which are typically grazed by microzooplankton. Copepods cannot effectively graze on phytoplankton particles below a threshold size. This size can vary with taxa and stage e.g., *Acartia tonsa*, a small copepod, was limited by 2-4 µm size for all stages, with higher optimal particle sizes as development progressed (Berggreen et al., 1988); whereas, calanoid copepods have a slightly larger size threshold of ~5 µm (Gauld, 1966; Boyd, 1976). Some of the larger fraction Chl*a* could also be due to retention of mixotrophic (Chl*a* containing) microzooplankton on the filters, as was observed on the shelf during June-July 2008-2010 (Stoecker et al., 2014b). Accordingly, it is possible that the higher large-size fraction Chl*a* seen in warm years is related to a combination of higher abundances of mixotrophic microzooplankton and reduced abundances of large zooplankton predators.

Variations in late summer/early fall Chl*a* were seen both interannually and between temperature regimes. Warm years generally had higher mean values than cold years, but significantly higher Chl*a* was only seen immediately north of the Alaska Peninsula, near St. Matthew Island and in the south-outer shelf. Currents at the moorings on the middle shelf vary between warm and cold conditions (Stabeno et al, this issue) but it is unclear whether differences in the currents are responsible for the differences in Chl*a*. The higher Chl*a* in warm years was due to large and small phytoplankton taxa in the south-outer shelf and near St. Mathew Island and due to large taxa north of the Alaska Peninsula. Large-size phytoplankton Chl*a* also was significantly higher in the south middle shelf (Regions 3 and 6) in warm years, suggesting changes in phytoplankton community composition, although the total Chl*a* was similar for both temperature regimes. This suggests that as the climate warms, phytoplankton biomass and community composition changes may be observed only in specific regions, not over the entire shelf. Some of the lack of significance is due to the high variability among years within a temperature regime.

Phytoplankton Chl*a* also had strong interannual variations, largely associated with variations in wind mixing and stratification. The high Chl*a* observed in 2005 over the southern middle shelf were in part related to the high August wind mixing that was observed up to 2 weeks prior to sampling (Table 4). At M2 in the south-middle domain, the breakdown of stratification occurred early (mid-October) in 2005 (Ladd and Stabeno, 2012), likely in part related to early wind mixing events. The bottom temperatures in the south-middle domain were also high in 2005, so a combination of high wind mixing and high bottom temperatures (the two most important factors explaining variability in integrated total Chl*a*) led to the anomalously high Chl*a*. In contrast, 2007 was the year with the lowest total and large-fraction Chl*a* and was a year with high stratification, low summer (June-August) wind mixing and anomalously low surface silicic acid (which may be an indicator of surface nutrient input during summer, Gann et al., this issue). The lack of surface nutrients, at least in part due to high stratification and low wind mixing, may have led to lower Chl*a* in 2007, with >80% of the community found in the small size (< 10 µm) fraction.

*4.3 Implications for fisheries*

Forage fish data (Parker-Stetter et al., this issue) were collected concurrently with zooplankton (Eisner et al., 2014) and hydrographic data (current study) during late summer/early fall in the eastern Bering Sea. Strong cross-shelf variations were observed for all three trophic levels: phytoplankton Chl*a* and size structure, zooplankton community structure and forage fish distributions (age-0 Walleye Pollock, Capelin (*Mallotus villosus*) and age-0 Pacific Cod). Fish distributions were most strongly related to water temperature and bottom depth, and secondarily to zooplankton prey (age-0 pollock only); however, there were no direct relationships to Chl*a* at the time of sampling. This is not unexpected, since there are temporal lags between primary, secondary and higher trophic level production. In situ water temperature, important for all three trophic levels, may relate to direct effects on growth or temperature tolerances, or may be indicative of other environmental factors associated with changes in temperature or larger scale ecosystem variations (Eisner et al., 2014, Parker-Stetter et al., this issue).

Low age-0 pollock weights and lengths were associated with low Chl*a* and primary production, low surface silicic acid and small phytoplankton cells in August/September 2007 in the southeast Bering Sea (Gann et al., this issue). We speculate that high stratification and low wind mixing

may have limited summer primary production, resulting in less trophic production reaching age-0 pollock. The small size of these pollock likely led to poor overwinter survival since recruitment to age-1 was low (Heintz et al., 2013). Thus, variations in summer phytoplankton production and Chl*a* can affect the ecosystem at distant trophic levels and may impact over-winter survival of forage fish and subsequent recruitment into the fishery.

### *4.4 Estimations of fall bloom timing*

The timing of our BASIS surveys in relation to fall storm events and stratification breakdown (mixing to bottom) may confound some of our interpretation, since the timing of decreases in stratification determines when nutrients are mixed to the surface to fuel the fall phytoplankton bloom. At M2, stratification breakdown (complete water column mixing) occurred during mid to late October in 2003-2005 (the three warm years), mid to late November in 2006-2008, late September to early October in 2009, with timing unknown for 2010-2012 (Ladd and Stabeno, 2012); although the start of fall mixing is earlier than breakdown. The average timing of the fall bloom at M2 was in late September based on mooring fluorometer data (Sigler et al., 2014); this is typically later than our surveys occurred in Region 3, indicating that we primarily sampled during late summer conditions (Table 1). MODIS data near M2 and M4 indicated that the highest fall Chl*a* occurred in September and October during 2002-2012, and SeaWIFS data over the shelf indicated highs in October for 2000-2010 (Liu et al., this issue). Our shelf-wide surveys ended by late September or early October, so we did not sample during the October bloom period. We could not adequately evaluate the timing of the fall blooms at higher resolution scales (8-day or bi-weekly), due to high cloud cover in this region, which reduced the number of pixels available for averaging MODIS data (<50% of the area could be evaluated consistently). Improved algorithms for ocean color measurements that account for variations in colored dissolved organic matter (CDOM) in the Bering Sea might improve the accuracy of our Chl*a* estimations (Naik et al., 2013), although estimations will still be severely hindered by the lack of cloud free days.

## 5. Summary

The large spatial and temporal variability in phytoplankton Chl*a* over the eastern Bering Sea in late summer/early fall is partially driven by spatial and temporal variations in nutrient inputs. Regions with consistently high values are associated with onshore transport of nutrients through bathymetric features such as canyons (e.g., near Pribilof Islands) or nutrient-rich currents (e.g. north of St. Lawrence Island). Chl*a* was positively associated with wind-mixing that occurred on average 2 weeks prior. This lag allows time for surface water to re-stratify and phytoplankton to undergo exponential growth. This process is important on the southeast middle shelf where nutrient concentrations are depleted in the surface, but are high at depth. In contrast, wind mixing during late summer/early fall will have little effect on Chl*a* on the northern shelf where deep nutrients are in low concentrations. Bottom temperature, associated with variations in sea ice and the cold pool extent, also has a positive relationship to Chl*a*. This may be related to larger ecosystem changes (e.g., variations in zooplankton communities and grazing pressure) that are set earlier in the growing season; however, the mechanisms are unknown. Bottom-up factors such as direct temperature effects on growth or increases in nutrients in the bottom pool could be relevant. Increases in Chl*a* in the warm, low ice years were greatest in the southeastern Bering Sea, with significant increases observed over the middle and outer shelf. These Chl*a* increases were due at least partially to increases in the large-size fraction phytoplankton (changes in phytoplankton community structure), perhaps due to changes in grazing pressure. The south-middle domain is highly impacted by reduction in sea ice, and zooplankton community structure (Stabeno et al., 2012b; Eisner et al., 2014), so large variations in Chl*a* there, are not unexpected. In the south-outer domain, additional factors may be driving changes in Chl*a* between temperature regimes; this area has lower variability in water temperature and zooplankton community structure, than seen in the middle shelf (Stabeno et al. 2012a; Eisner et al. 2014). Reductions in southerly sea ice extent and subsequent increases in water temperature associated with a warming climate may lead to increases in phytoplankton total and large-size fraction Chl*a* in the southeastern Bering Sea, but interannual variability in local wind mixing and stratification, uncorrelated with temperature regime changes in the current study, will continue to be important factors driving variations in biomass in stratified regions during summer.

## Acknowledgements

We are grateful to the captains and crews of the NOAA ship *Oscar Dyson*, and charter vessels, *Sea Storm*, *NW Explorer*, and *Epic Explorer*, and *Bristol Explorer* for their years of hard work and diligence on our surveys. We appreciate the assistance in field sampling, data processing and analysis from NOAA scientific staff and volunteers. In particular, we appreciate the help from J. Lanksbury, J. Pohl, and F. Van Tulder for analysis of numerous chlorophyll samples. J. Lanksbury also assisted with database management. We thank S. Danielson for assistance with QA and processing of CTD data. Kathy Krogslund Lab (UW) and C. Mordy Lab (PMEL) provided processing of nutrient samples. We thank N. Bond for NCEP re-analysis wind data and S. Salo for MODIS ocean color data retrieval (via NOAA CoastWatch Program and NASA's Goddard Space Flight Center, OceanColor Web). We thank K. Mier for guidance on statistical analyses. We greatly appreciate the helpful comments from M. Sigler on an earlier version of this manuscript and edits and suggestions provided by the special edition editor, M. Lomas, and four anonymous reviewers. Funding was provided by the North Pacific Research Board (NPRB), Bering Sea Fisherman's Association, Arctic-Yukon-Kuskokwim-Sustainable-Salmon-Initiative, Coastal Impacts Assistance Program (CIAP), Bureau of Ocean Energy Management (BOEM), and NOAA National Marine Fisheries Service including the Fisheries and the Environment (FATE) Program. This research is contribution 4164 to PMEL, contribution EcoFOCI-0822 to NOAA's Ecosystems and Fisheries-Oceanography Coordinated Investigations, Bering Sea Project publication number 160 and NPRB publication number 539. The findings and conclusions in the paper are those of the author(s) and do not necessarily represent the views of the National Marine Fisheries Service. Reference to trade names does not imply endorsement by the National Marine Fisheries Service, NOAA.

## References


Baier, C.T. Napp, J.M., 2003. Climate-induced variability in *Calanus marshallae* populations. J. Plankton Res. 25, 771-782.

Berggreen, U., Hansen, B., Kiorboe, T., 1988. Food size spectra, ingestion and growth of the copepod during development: implications for determination of copepod production. Mar. Biol. 99, 341-352.

Bond, N.A., Adams, J.M., 2002. Atmospheric forcing of the southeast Bering Sea Shelf during 1995-99 in the context of a 40-year historical record. Deep-Sea Res. II 49, 5869-5887.

Boyd, C.M., 1976. Selection of particle sizes in filter-feeding copepods: A plea for reason. Limnol. Oceanogr. 21, 175-180.

Brown, Z.W., Arrigo, K.R., 2013. Sea ice impacts on spring bloom dynamics and net primary production in the eastern Bering Sea. J. Geophys. Res. 118, 1-20.

Brown, Z.W., van Dijken, G.L., Arrigo, K.R., 2011. A reassessment of primary production and environmental change in the Bering Sea. J. Geophys. Res. 116, C08014.

Byrd, G.V., Schmutz, J.A., Renner, H.A., 2008. Contrasting population trends of piscivorous seabirds in the Pribilof Islands: A 30-year perspective. Deep Sea Res. II 55(16-17), 1846-1855.

Call, K. A., Ream, R.R., Johnson, D. Sterling, J.T., Towell, R.G., 2008. Foraging route tactics and site fidelity of adult female northern fur seal (*Callorhinus ursinus*) around the Pribilof Islands. Deep Sea Res. II 55(16-17), 1883-1896.

Coachman, L.K., 1986. Circulation, water masses and fluxes on the southeastern Bering Sea shelf. Cont. Shelf Res. 5, 23–108.

Coyle, K.O., Eisner, L.B., Mueter, F.J., Pinchuk, A.I., Janout, M.A., Cieciel, K.D., Farley, E.V., Andrews, A.G., 2011. Climate change in the southeastern Bering Sea: impacts on pollock stocks and implications for the oscillating control hypothesis. Fish. Oceanogr. 20, 139–156.

Coyle, K.O., Pinchuk, A.I., Eisner, L.B., Napp, J.M., 2008. Zooplankton species composition, abundance and biomass on the eastern Bering Sea shelf during summer: the potential role of water column stability and nutrients in structuring the zooplankton community. Deep Sea Res. II 55, 1775–1791.

Danielson, S., Eisner, L., Weingartner, T., Aagaard, K., 2011. Thermal and haline variability over the central Bering Sea shelf: Seasonal and interannual perspectives Cont. Shelf Res. 31, 539-554. doi:10.1016/j.csr.2010.12.010.

Danielson, S., Hedstrom, K., Aagaard, K., Weingartner, T., Curchitser, E., 2012. Wind-induced reorganization of the Bering shelf circulation. Geophys. Res. Lett. 39, L08601. 10.1029/2012gl051231.

Duffy-Anderson, J., Busby, Mier, K. L., Deliyanides, C. M., Stabeno, P. J., 2006. Spatial and temporal patterns in summer ichthyoplankton assemblages on the eastern Bering Sea shelf 1996-2000. Fish. Oceanogr. 15(1), 80-94.

Eisner, L., Napp, J., Mier, K., Pinchuk, A., Andrews A., 2014. Climate-mediated changes in zooplankton community structure for the eastern Bering Sea. Deep Sea Res. II http://dx.doi.org/10.1016/j.dsr2.2014.03.004.

Eppley, R.W., 1972. Temperature and phytoplankton growth in the sea. Fish Bull. 70(4), 1063-1085.

ESRI, 2014. ArcGIS Desktop: Release 10.2.2 Redlands, CA: Environmental Systems Research Institute.

Gann, J.C., Eisner, L.B., Porter, S., Watson, J.T., Cieciel, K.D., Mordy, C.W., Yasumiishia, E.M., Stabeno, P.J., Ladd, C., Heintz, R.A., Farley, E.V., this issue. Possible mechanism linking ocean conditions to low body weight and poor recruitment of age-0 walleye pollock (*Gadus chalcogrammus*) in the southeast Bering Sea during 2007. Deep Sea Res. II.

Gauld, D.T., 1966. The swimming and feeding of planktonic copepods, In: H. Barnes (ed.) Some contemporary studies in marine science. Allen and Unwin, London, p. 313-334.

Goering, J.J., Iverson, R.L., 1981. Phytoplankton distribution on the southeastern Bering Sea shelf. In: D.W. Hood and J.A Calder (eds.) The eastern Bering Sea shelf: oceanography and resources. Vol. 2, 933-946.

Granger, J, Prokopenko, M.G., Mordy, C.W., Sigman, D.M., 2013. The proportion of remineralized nitrate on the ice-covered eastern Bering Sea shelf evidenced from the oxygen isotope ratio of nitrate. Global Biogeochem. Cycles, 27(3), 962–971. doi: 10.1002/gbc.20075.

Grasshoff, K., 1976. Methods of seawater analysis. Verlag Chemie, Weinheim, New York.

Grebmeier, J.M., Cooper, L.W., Feder, H.M., Sirenko, B.I., 2006. Ecosystem Dynamics of the Pacific-Influenced Northern Bering and Chukchi Seas. Progress in Oceanography, 71: 331-361.

Hansell, D.A., Whitledge, T.E., Goering, J.J., 1993. Patterns of nitrate utilization and new production over the Bering–Chukchi Shelf. Cont. Shelf Res., 13(5-6): 601-627.

Heintz, R.A., Siddon, E.C., Farley E.V., Napp, J.M., 2013. Correlation between recruitment and fall condition of age-0 pollock (*Theragra chalcogramma*) from the eastern Bering Sea under varying climate conditions. Deep Sea Res. II 94,150-156.

Hunt, G.L., Stabeno, P.J., Strom, S., Napp, J.M., 2008. Patterns of spatial and temporal variation in the marine ecosystem of the southeastern Bering Sea, with special reference to the Pribilof Domain. Deep Sea Res. II 55, 1919–1944.

ICES, 2004. Chemical measurements in the Baltic Sea: Guidelines on quality assurance. In: E. Lysiak-Pastuszak and M. Krysell (eds.) ICES Techniques in Marine Environmental Sciences. No. 35. 149 pp.

Jahncke, J., Vlietstra, l.S., Decker, M.B., Hunt, G.L., 2008. Marine bird abundance around the Pribilof Islands: A multiyear comparison. Deep Sea Res. II 55, 1809-1826.

JGOFS, 1994. Protocols for the joint global ocean flux study (JGOFS) core measurements. IOC, Scientific Committee on Oceanic Research. Manuals and Guides. Vol. 29, Paris, France, UNESCO Publishing, 170 p.

Kachel, N.B., Hunt Jr., G.L., Salo, S.A., Schumacher, J.D., Stabeno, P.J., Whitledge, T.E., 2002. Characteristics and variability of the inner front of the southeastern Bering Sea. Deep Sea Res. II 49 (26), 5889–5909.

Kalnay, E., Kanamitsu, M., Kistler, R., Collins, W., Deaven, D., Gandin, L., Iredell, M., Saha, S., White, G., Woollen, J., Zhu, Y., Leetmaa, A., Reynolds, B., Chelliah, M., Ebisuzaki, W., Higgins, W., Janowiak, J., Mo, K.C., Ropelewski, C., Wang, J., Jenne, R., Joseph, D., 1996. The NCEP/NCAR 40-Year Reanalysis Project. Bull. Amer. Meteor. Soc. 77, 437–472.

Kinney, J.C., Maslowski, W., Okkonen, S., 2009. On the processes controlling shelf-basin exchange and outer shelf dynamics in the Bering Sea. Deep-Sea Res. II 56, 1351-1362, doi:10.1016/j.dsr2.2008.10.023.

Kopylov, A.I.. Flint. M.V., Drits. A.V., 2002. Primary production of phytoplankton in the eastern part of the Bering Sea. Oceanol. 42, 215-225.

Ladd C., Stabeno, P.J., 2012. Stratification on the Eastern Bering Sea shelf revisited. Deep Sea Res. II 65-70, 72-83.

Lomas, M.W., Moran, S.B., Casey, J.R., Bell, D.W., Tiahlo, M., Whitefield, J., Kelly, R.P., Mathis, J.T., Cokelet, E.D., 2012. Spatial and seasonal variability of primary production on the eastern Bering Sea shelf. Deep Sea Res. II 65-70, 126-140.

Liu, C. L., Zhai L., Zeeman, S.I., Eisner, L.B., Gann, J., Mordy, C.W. Moran, S.B., Lomas, M.W., this issue. Seasonal and geographic variations in modeled primary production and

phytoplankton losses from the mixed layer between warm years and cold years on the eastern Bering Sea shelf. Deep Sea Res. II.

Mantoura, R.F.C., Woodward, E.M.S., 1983. Optimization of the indophenol blue method for the automated determination of ammonia in estuarine waters. Estuar. Coast. Shelf Sci. 17, 219–224.

McCormick-Ray, J., Warwick, R.M., Ray, G.C. 2011. Benthic macrofaunal compositional variations in the northern Bering Sea. Mar Biol. 158, 1365-1376.

McRoy, C.P . Goering, J. J., Shiels, W.E., 1972. Studies of primary production in the eastern Bering Sea. In: Takenouti, A.Y. (Ed.), Biological Oceanography of the Northern North Pacific Ocean. Idemitsu Shoten, Tokyo, p. 199-216.

Moran, S.B., Lomas, M.W., Kelly, R.P., Gradinger, R., Iken, K., Mathis, J.T., 2012. Seasonal succession of net primary productivity, particulate organic carbon export, and autotrophic community composition in the eastern Bering Sea. Deep Sea Res. II 65-70, 84-97.

Mordy, C.W., Cokelet, E.D., Ladd, C., Menzia, F.A., Proctor, P., Stabeno, P.J., Wisegarver, E., 2012. Net community production on the middle shelf of the eastern Bering Sea. Deep Sea Res. II 65-70, 110-125.

Mordy, C.W., Eisner, L.B., Proctor, P., Stabeno, P., Devol, A.H., Shull, D.H., Napp, J.M., Whitledge, T., 2010.Temporary uncoupling of the marine nitrogen cycle: Accumulation of nitrite on the Bering Sea shelf. Mar. Chem. 121, 157166.

Mordy, C.W., Stabeno, P.J., Ladd, C., Zeeman, S., Wisegarver, D.P., Hunt, G.L., Jr., 2005. Nutrients and primary production along the eastern Aleutian Island Archipelago. Fish. Oceanogr. 14, 55-76.

Mordy, C.W., Stabeno, P.J., Righi, D., Menzia, F.A., 2008. Origins of the subsurface ammonium maximum in the southeast Bering Sea. Deep-Sea Res. II, 55, 1738-1744.

Naik, P., D'Sa, E.J., Gomes, H.R., Goés, J.I., Mouw, C.B., 2013. Light absorption properties of southeastern Bering Sea waters: Analysis, parameterization and implications for remote sensing. Remote Sensing of Environment 134, 120–134.

Olson, M.B., Strom, S.L., 2002. Phytoplankton growth, micro-zooplankton herbivory and community structure in the southeast Bering Sea: insight into the formation and temporal persistence of an *Emiliania huxleri* bloom. Deep-Sea Res. II 49, 5969-5990.

Ortiz, I,. Wiese, F., Greig, A., 2012. Marine regions boundary data for the Bering Sea shelf and slope. UCAR/NCAR - Earth Observing Laboratory/Computing, Data, and Software Facility. Dataset. doi:10.5065/D6DF6P6C.

Parker-Stetter, S., Urmy, S., Horne, J., Eisner, L., Farley, E., this issue. Factors affecting summer distributions of Bering Sea forage fish species: assessing competing hypotheses. Deep-Sea Res. II.

Parsons, T.R., Maita, Y., Lalli, C.M., 1984. A Manual of Chemical and Biological Methods for Seawater Analysis. Pergamon Press, Oxford, England, 173 pp.

Ressler, P.H., De Robertis, A., Warren, J.D., Smith, J.N., Kotwicki, S., 2012. Developing an acoustic survey of euphausiids to understand trophic interactions in the Bering Sea ecosystem, Deep Sea Res. II 65–70,184-195.

Rho, T., Whitledge, T.E., 2007. Characteristics of seasonal and spatial variations of primary production over the southeastern Bering Sea shelf. Cont. Shelf Res. 27, 2556-2569.

Sambrotto, R.N. Goering, J.J., 1983. Interannual variability of phytoplankton and zooplankton production on the southeast Bering Sea shelf. In From Year to Year. W.S. Wooster (ed.) Washington Sea Grant, Seattle, pp161-177.

Sambrotto, R.N., Goering, J.J, McRoy ,C.P., 1984. Large yearly production of phytoplankton in the western Bering Strait. Science 225,1147-1150.

Sambrotto, R.N., Mordy, C.W., Zeeman, S.I., Stabeno, P.J., Macklin, S.A., 2008. Physical forcing and nutrient conditions associated with patterns of Chl *a* and phytoplankton productivity in the southeastern Bering Sea during summer. Deep Sea Res. II 55, 1745–1760.

Sambrotto R.N., Niebauer, H.J., Goering, J.J., Iverson, R.L., 1986. Relationships among vertical mixing nitrate uptake and phytoplankton growth during the spring bloom in the southeast Bering Sea middle shelf. Cont. Shelf Res. 5, 161–198.

Siddon, E.C., Heintz, R.A., Meuter F.J., 2013. Conceptual model of energy allocation in Walleye Pollock (*Theragra chalcogramma*) from larvae to age-1 in the eastern Bering Sea. Deep Sea Res. II 94,140-149.

Sigler, M.F., Heintz, R.A., Hunt, G.L., Lomas, M.W., Napp, J. M., Stabeno, P., this issue. A mid-trophic view of subarctic productivity: lipid storage, location matters and historical context. Deep-Sea Res. II.

Sigler, M.F., Stabeno, P., Eisner, L.B., Napp, J. M., Mueter, F.J., 2014. Spring and fall phytoplankton blooms in a productive subarctic ecosystem, the eastern Bering Sea, during 1995-2011. Deep-Sea Res. II, http://dx.doi.org/10.1016/j.dsr2.2013.12.007.

Simpson, J.H., Hughes, D.G., Morris, N.C.G., 1977. The relation of seasonal stratification to tidal mixing on the continental shelf. Deep Sea Res. 24(Suppl.), 327–340.

Slawyk, G., MacIsaac, J.J., 1972, Comparison of two automated ammonium methods in a region of coastal upwelling, Deep Sea Res.19, 521-524.

Springer, A.M., McRoy, C.P., 1993. The paradox of pelagic food webs in the northern Bering Sea- III. Patterns of primary production.

Springer, A.M., McRoy, C.P., Flint M.V., 1996. The Bering Sea Green Belt: shelf-edge processes and ecosystem production. Fish. Oceanogr. 5, 205- 223.

Stabeno, P.J., Bond, N.A., Kachel, N.B., Salo, S.A., Schumacher, J.D., 2001. On the temporal variability of the physical environment over the south-eastern Bering Sea. Fish. Oceanogr. 10, 81-98.

Stabeno, P.J., Danielson, S., Kachel, D., Kachel, N.B., Mordy, C.W., this issue. Currents and transport on the Eastern Bering Sea shelf. Deep-Sea Res. II.

Stabeno, P.J., Farley, E.V., Kachel, N., Moore, S., Mordy, C., Napp, J.M., Overland, J.E., Pinchuk, A.I., Sigler, M., 2012a. A comparison of the physics, of the northern and southern shelves of the eastern Bering Sea and some implications to the ecosystem. Deep Sea Res. II 65-70:14-30.

Stabeno, P.J., Kachel, N.B., Moore, S.E., Napp, J.M., Sigler, M., Yamaguchi, A., Zerbini, A.N., 2012b. Comparison of warm and cold years on the southeastern Bering Sea shelf and some implications for the ecosystem. Deep Sea Res. II 65-70:31-45.

Stabeno, P. J., Kachel, N., Mordy, C., Righi, D., Dalo, S., 2008. An examination of the physical variability around the Pribilof Islands in 2004. Deep Sea Res. II 55(16-17), 1701-1716.

Stabeno, P.J., Napp, J., Mordy, C., Whitledge, T., 2010. Factors influencing physical structure and lower trophic levels of the eastern Bering Sea shelf in 2005: sea ice, tides and winds. Prog. Oceanogr. 85 (3-4), 180–196.

Stabeno, P.J., Reed, R.K., Napp, J.M., 2002. Transport through Unimak pass, Alaska. Deep Sea Res. II 49, 5919-5930.

Stoecker, D.A. Weigel, A., Goes, J.I., 2014a. Microzooplankton grazing in the eastern Bering Sea in summer, Deep Sea Res. II, http://dx.doi.org/10.1016/j.dsr2.2013.09.017.

Stoecker, D.K., Weigel, A.C., Stockwell, D.A., Lomas, M.W., 2014b. Microzooplankton: Abundance, biomass and contribution to chlorophyll in the eastern Bering Sea in summer. Deep Sea Res. II, http://dx.doi.org/10.1016/j.dsr2.2013.09.007.

Strom, S.L., Fredrickson, K.A., 2008. Intense stratification leads to phytoplankton nutrient limitation and reduced microzooplankton grazing in the southeastern Bering Sea. Deep Sea Res. II 55(16-17), 1761-1774.

Sullivan, M.E., Kachel, N.B., Mordy, C.W., Stabeno, P.J., 2008. The Pribilof Islands: Temperature, salinity and nitrate during summer 2004. Deep Sea Res. II 55(16-17), 1729-1737.

Systat Software, Inc., 2009. For Windows, Version 13, San Jose, CA.

Walsh, J.J., McRoy, C.P., Coachman, L.K., Goering, J.J., Nihoul, J.J., Whitledge, T.E., Blackburn, T.H., Parker, P.L., Wirick, C.D., Shuert, P.G., Grebmeier, J.M., Springer, A.M., Tripp, R.D., Hansell, D.A., Djenidi, S., Deleersnijder, E., Henriksen, K., Lund, B.A., Andersen, P., Mullerkarger, F.E., Dean, K., 1989. Carbon and nitrogen cycling within the Bering Chukchi Seas - source regions for organic-matter effecting AOU demands of the Arctic Ocean. Prog. Oceanogr. 22, 277-359.

Whitledge, T.E., Reeburgh, W.S., Walsh, J.J., 1986. Seasonal inorganic nitrogen distributions and dynamics in the southeastern Bering Sea Cont. Shelf Res. 5, 109–132.

Wiese, F.K., Wiseman, W.J., van Pelt, T.I., 2012. Bering Sea linkages. Deep Sea Res. II 65-70, 2-5.

Zador, S., 2014. Ecosystem Considerations 2014, Stock Assessment and Fishery Evaluation Report, North Pacific Fisheries Management Council, 605 W 4th Ave, Suite 306, Anchorage, AK 99501.

Table 1. BASIS survey dates for entire shelf and Region 3.

| | Entire shelf | | Region 3 | |
|---|---|---|---|---|
| year | start | end | start | end |
| 2003 | 21-Aug | 8-Oct | 2-Sep | 23-Sep |
| 2004 | 14-Aug | 30-Sep | 16-Aug | 4-Sep |
| 2005 | 14-Aug | 6-Oct | 15-Aug | 13-Sep |
| 2006 | 18-Aug | 20-Sep | 20-Aug | 3-Sep |
| 2007 | 15-Aug | 8-Oct | 16-Aug | 13-Sep |
| 2008 | 11-Sep | 27-Sep | 12-Sep | 26-Sep |
| 2009 | 30-Aug | 27-Sep | 4-Sep | 27-Sep |
| 2010 | 18-Aug | 4-Oct | 19-Aug | 16-Sep |
| 2011 | 21-Aug | 19-Sep | 24-Aug | 19-Sep |
| 2012 | 19-Aug | 12-Oct | 24-Aug | 13-Sep |

Table 2. Means of (A) integrated total Chl*a*, (B) integrated Chl*a* > 10 µm (mg $m^{-2}$), and (C) number of stations sampled by region and year. Standardized anomaly calculated on natural log transformed data and standardized to maximum. Color coding indicates if anomaly is negative (red, -1 to -0.3), small (yellow, -0.3 to 0.3) or positive (green, 0.4 to 1). Means for each region for all years combined are shown in the last column in panels A and B. *Intended for color reproduction on the Web and in print.*

(A)

| Domain | Region | | 2003 | 2004 | 2005 | 2006 | 2007 | 2008 | 2009 | 2010 | 2011 | 2012 | Mean |
|---|---|---|---|---|---|---|---|---|---|---|---|---|---|
| Inner | South | **2** | 55 | 65 | 86 | 56 | 42 | 26 | 40 | 65 | 57 | 55 | 55 |
| | Mid-north | **7** | 59 | 60 | 63 | 44 | 15 | 41 | 40 | 48 | 50 | 40 | 46 |
| | North | **11** | 34 | 52 | 45 | 19 | 23 | | 36 | 46 | 58 | 36 | 39 |
| Middle | AK Penn | **1** | 75 | 86 | 136 | 48 | 38 | 34 | 58 | 51 | 62 | 50 | 64 |
| | South | **3** | 67 | 67 | 112 | 47 | 26 | 32 | 55 | 42 | 71 | 62 | 58 |
| | Pribilofs | **5** | | 217 | 178 | 39 | 52 | | 53 | | 243 | 79 | 123 |
| | Mid-north | **6** | 115 | 79 | 118 | 42 | 48 | 29 | 69 | 39 | 76 | 77 | 69 |
| | St Matthew | **9** | 77 | 86 | 85 | 32 | 43 | | 56 | 29 | 60 | 42 | 57 |
| | North | **10** | | 50 | 55 | 17 | 23 | | 17 | 37 | 66 | 15 | 35 |
| Outer | South | **4** | 85 | 75 | 121 | 65 | 61 | 29 | 64 | 46 | 55 | 77 | 68 |
| > 63°N | St Lawrence | **12** | 32 | 60 | | 1 | 29 | | 88 | 58 | 81 | 32 | 48 |
| | S Bering Strait | **13** | 73 | 32 | 18 | 35 | 39 | | 54 | 41 | 69 | 96 | 51 |
| | Norton Sound | **14** | 9 | 31 | 14 | 9 | 36 | | 25 | 43 | 53 | 26 | 27 |
| Offshore | southeast | **16** | 92 | 113 | 137 | 80 | | | | 315 | 174 | | 152 |

(B)

| Domain | Region | | 2003 | 2004 | 2005 | 2006 | 2007 | 2008 | 2009 | 2010 | 2011 | 2012 | Mean |
|---|---|---|---|---|---|---|---|---|---|---|---|---|---|
| Inner | South | **2** | 31 | 23 | 51 | 21 | 10 | 8 | 13 | 39 | 33 | 15 | 24 |
| | Mid-north | **7** | 49 | 33 | 40 | 13 | 5 | 7 | 14 | 30 | 32 | 15 | 24 |
| | North | **11** | 19 | 26 | 34 | 8 | 10 | | 13 | 19 | 30 | 18 | 20 |
| Middle | AK Penn | **1** | 31 | 39 | 82 | 8 | 9 | 3 | 16 | 14 | 19 | 25 | 25 |
| | South | **3** | 32 | 32 | 70 | 11 | 4 | 4 | 16 | 13 | 16 | 15 | 21 |
| | Pribilofs | **5** | | 60 | 131 | 24 | 20 | | 10 | | 129 | 44 | 60 |
| | Mid-north | **6** | 41 | 50 | 85 | 18 | 12 | 12 | 24 | 10 | 30 | 41 | 32 |
| | St Matthew | **9** | 36 | 40 | 40 | 9 | 17 | | 13 | 9 | 25 | 25 | 24 |
| | North | **10** | | 20 | 29 | 4 | 5 | | 5 | 11 | 26 | 4 | 13 |
| Outer | South | **4** | 16 | 16 | 55 | 10 | 8 | 4 | 10 | 3 | 5 | 38 | 17 |
| >63°N | St Lawrence | **12** | | 38 | | 0 | 16 | | 102 | 5 | 13 | 1 | 25 |
| | S Bering Strait | **13** | 1 | 12 | 10 | 21 | 16 | | 29 | 10 | 34 | 61 | 21 |
| | Norton Sound | **14** | 5 | 10 | 7 | 4 | 11 | | 6 | 24 | 31 | 10 | 12 |
| Off shelf | southeast | **16** | 38 | 30 | 67 | 17 | | | | 208 | 135 | | 82 |

(C)

| Domain | Region | | 2003 | 2004 | 2005 | 2006 | 2007 | 2008 | 2009 | 2010 | 2011 | 2012 | Total |
|---|---|---|---|---|---|---|---|---|---|---|---|---|---|
| Inner | South | **2** | 14 | 16 | 16 | 13 | 12 | 7 | 7 | 14 | 10 | 12 | 65 |
| | Mid-north | **7** | 4 | 9 | 9 | 9 | 9 | 3 | 3 | 8 | 4 | 8 | 121 |
| | North | **11** | 8 | 16 | 15 | 12 | 14 | | 14 | 15 | 15 | 13 | 199 |
| Middle | AK Penn | **1** | 8 | 7 | 8 | 6 | 6 | 3 | 4 | 8 | 7 | 8 | 72 |
| | South | **3** | 15 | 23 | 21 | 24 | 23 | 13 | 13 | 22 | 21 | 24 | 17 |
| | Pribilofs | **5** | | 2 | 2 | 3 | 3 | | 1 | | 3 | 3 | 95 |
| | Mid-north | **6** | 6 | 10 | 5 | 13 | 13 | 4 | 7 | 12 | 12 | 13 | 66 |
| | St Matthew | **9** | 4 | 6 | 7 | 5 | 7 | | 5 | 7 | 6 | 3 | 50 |
| | North | **10** | | 10 | 10 | 10 | 9 | | 10 | 9 | 9 | 1 | 68 |
| Outer | South | **4** | 3 | 7 | 9 | 6 | 10 | 1 | 7 | 10 | 10 | 9 | 122 |
| >63°N | St Lawrence | **12** | 2 | 2 | | 2 | 2 | | 2 | 1 | 2 | 1 | 14 |
| | S Bering Strait | **13** | 5 | 7 | 4 | 7 | 8 | | 8 | 9 | 9 | 9 | 66 |
| | Norton Sound | **14** | 4 | 4 | 1 | 4 | 2 | | 5 | 6 | 6 | 6 | 38 |
| Off shelf | southeast | **16** | 1 | 1 | 1 | 1 | | | | 1 | 1 | | 6 |
| | | Total | 74 | 120 | 108 | 115 | 118 | 31 | 86 | 122 | 115 | 110 | 999 |

Table 3. Statistical differences between regimes (warm and cold years) for integrated Chl*a* (total, large (> 10 µm), and small (< 10 µm) size fractions, natural log transformed), and temperature and salinity above (surface) and below (deep) the pycnocline by region. Results show Type III Tests for Fixed Effects for Regime using Hierarchical Mixed Model with REML estimation in SYSTAT. The * indicates significantly ($P < 0.05$) higher values in warm years.

| | | | **Int Chla total** | **Int Chla large** | **Int Chla small** | **T surface** | **T deep** | **S surface** | **S deep** |
|---|---|---|---|---|---|---|---|---|---|
| Domain | Region | | P-value | P-value | P-value | P-value | P-value | P-value | P-value |
| Inner | South | 2 | 0.099 | 0.142 | 0.507 | 0.001 * | 0.000 * | 0.836 | 0.456 |
| | Mid-north | 7 | 0.153 | 0.061 | 0.976 | 0.022 * | 0.006 * | 0.124 | 0.183 |
| | North | 11 | 0.622 | 0.275 | 0.995 | 0.638 | 0.054 | 0.708 | 0.588 |
| Middle | AK Penn | 1 | 0.015 * | 0.022 * | 0.314 | 0.003 * | 0.002 * | 0.111 | 0.075 |
| | South | 3 | 0.149 | 0.014 * | 0.712 | 0.004 * | 0.001 * | 0.000 * | 0.029 * |
| | Pribilofs | 5 | 0.267 | 0.485 | 0.530 | 0.070 | 0.003 * | 0.002 * | 0.060 |
| | Mid-north | 6 | 0.094 | 0.020 * | 0.104 | 0.013 * | 0.000 * | 0.000 * | 0.001 * |
| | St Matthew | 9 | 0.010 * | 0.018 * | 0.015 * | 0.286 | 0.001 * | 0.003 * | 0.048 * |
| | North | 10 | 0.246 | 0.137 | 0.171 | 0.248 | 0.149 | 0.293 | 0.284 |
| Outer | South | 4 | 0.013 * | 0.037 * | 0.030 * | 0.074 | 0.001 * | 0.907 | 0.512 |
| > 63°N | St Lawrence | 12 | 0.354 | 0.979 | 0.443 | 1.000 | 0.561 | 0.675 | 0.782 |
| | S Bering St | 13 | 0.284 | 0.139 | 0.148 | 0.204 | 0.085 | 0.249 | 0.063 |
| | Norton S | 14 | 0.106 | 0.274 | 0.939 | 0.060 | 0.055 | 1.000 | 0.137 |

Table 4. August stratification index (J $m^{-2}$) and $u_*^3$ ($m^{-3}$ $s^{-3}$, an indicator of wind mixing), and number of summer (June-August) wind mixing events ($u_*^3$ > 0.05 $m^3$ $s^{-3}$) at M2 on the southeast middle shelf for 2003-2012. Bold indicates warm years; all other years were cold with the exception of 2006, which was average.

| Year | Stratification Index | $u_*^3$ | # Wind Mixing Events |
|---|---|---|---|
| **2003** | **5234** | **0.015** | **7** |
| **2004** | **6099** | **0.026** | **9** |
| **2005** | **5432** | **0.045** | **10** |
| 2006 | 4625 | 0.019 | 9 |
| 2007 | 6036 | 0.018 | 3 |
| 2008 | 4271 | 0.008 | 6 |
| 2009 | 4436 | 0.025 | 10 |
| 2010 | 4927 | 0.019 | 9 |
| 2011 | 5036 | 0.020 | 14 |
| 2012 | 4124 | 0.021 | 5 |
| Ave 1995-2012 | 4655 | | |
| SD 1995-2012 | 848 | | |

Table 5. Best fit environmental variables explaining interannual variation in integrated total and > 10 µm Chl*a* using GLM stepwise regressions for Region 3 (near M2) and Region 6 (near M4).

| Region 3 (M2) | P-value and direction | Region 6 (M4) | P-value and direction |
|---|---|---|---|
| Integrated Chl*a* total | | | |
| T deep | 0.001 (+) | T deep | 0.002 (+) |
| Aug $u_*^3$ | 0.001 (+) | Aug $u_*^3$ | 0.088 (+) |
| Aug stratification | 0.004 (−) | NA | NA |
| Adjusted multiple $r^2$ | 0.96 | | 0.86 |
| Integrated Chl*a* >10 µm | | | |
| T deep | 0.001 (+) | Aug $u_*^3$ | 0.003 (+) |
| Aug $u_*^3$ | 0.001 (+) | Ammonium deep | 0.059 (+) |
| Silicic acid deep | 0.015 (−) | | |
| Adjusted multiple $r^2$ | 0.96 | | 0.83 |

**Figure captions**

Figure 1. Stations within each Bering Sea Project Region (Ortiz et al., 2012) sampled a minimum of 5 years between 2003 and 2012. We sampled three inner shelf regions (Regions 2, 7, 11), six middle shelf regions (Regions 1, 3, 5, 6, 9, 10), one outer shelf region (Region 4) and three regions north and east of St. Lawrence Island (Regions 12, 13 and 14).

Figure 2. Contours of (A) integrated total Chl*a* and (B) integrated > 10 µm Chl*a* averaged over 2003-2012. Data integrated over the top 50 m. *Intended for color reproduction on the Web and in print.*

Figure 3. Contours of (A) surface nitrate ($NO_3$), (B) surface ammonium ($NH_4$), (C) surface dissolved inorganic nitrogen (DIN), (D) surface silicic acid (Si), (E) deep $NO_3$, (F) deep $NH_4$, (G) deep DIN, and (H) deep Si averaged over 2003-2012. Nutrients were collected at depths of 5 m (surface) and 30-60 m (deep). *Intended for color reproduction on the Web and in print.*

Figure 4. Contours of mean water column stratification index averaged over 2003-2009. Stars indicate locations of PMEL moorings, M2 and M4. *Intended for color reproduction on the Web and in print.*

Figure 5. Contours of data averaged over warm (2003-2005) years (top panel) and cold (2007-2012) years (bottom panel) for (A, E) integrated total Chl*a*, (B, F) integrated > 10 µm Chl*a*, (C, G) surface (above pycnocline) temperature, and (D, H) deep (below pycnocline) temperature. *Intended for color reproduction on the Web and in print.*

Figure 6. Linear regressions of mean integrated total Chl*a* and percent large-fraction Chl*a* (mean > 10 µm Chl*a* /total Chl*a*) from discrete samples averaged over the top 50 m for 2003-2012 for Regions 1 and 3 (south-middle), 4 (south-outer) and 10 (north-middle).

Figure 7. Linear regressions between integrated total Chl*a* and (A, B) $u_*^3$, a proxy of August wind mixing , (C, D) temperature below the pycnocline, and (E) August stratification for 2003-2012 for Regions 3 and 6.

Figure 8. (A) Mean Chl*a* (mg $m^{-3}$) from MODIS for 2002-2012 by Region (1, 3, 5, and 6) for August, September and October. * indicates October significantly lower than September in

Region 5, and August significantly lower than later months for Regions 3 and 6 ($P < 0.05$, ANOVA with Tukey tests). Errors bars show ± 1 standard error. (B) Chl*a* from MODIS for August, September, and October for Region 3 by year. Aug-Oct MODIS is the sum of Chl*a* from MODIS for all three months for each year. BASIS surface Chl*a* (~5 m) shown for comparison.

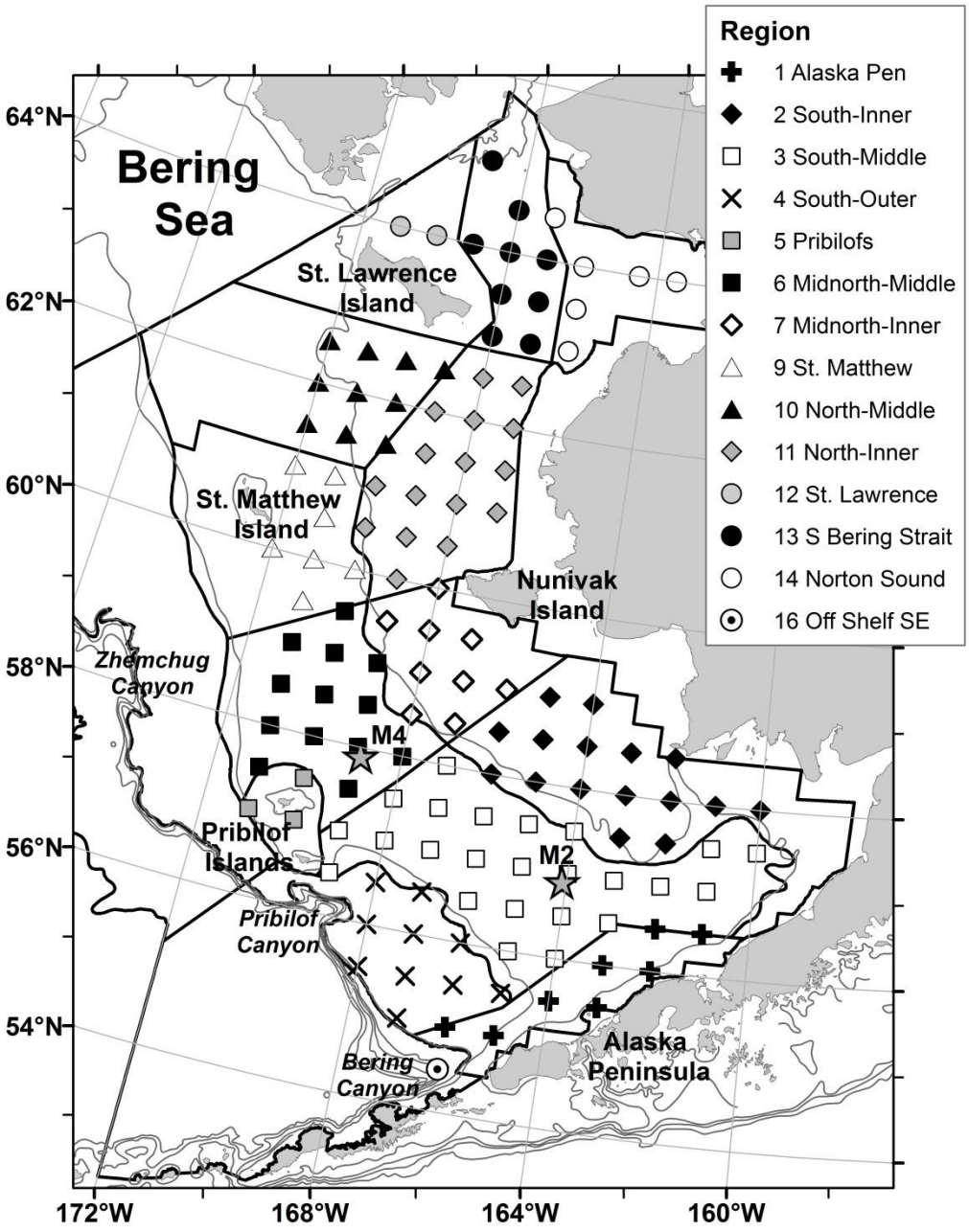
Region
1 Alaska Pen
2 South-Inner
3 South-Middle
4 South-Outer
5 Pribilofs
6 Midnorth-Middle
7 Midnorth-Inner
9 St. Matthew
10 North-Middle
11 North-Inner
12 St. Lawrence
13 S Bering Strait
14 Norton Sound
16 Off Shelf SE
Bering Sea
St. Lawrence Island
St. Matthew Island
Nunivak Island
Zhemchug Canyon
M4
M2
Pribilof Islands
Pribilof Canyon
Bering Canyon
Alaska Peninsula
64°N
62°N
60°N
58°N
56°N
54°N
172°W
168°W
164°W
160°W

Figure 1.

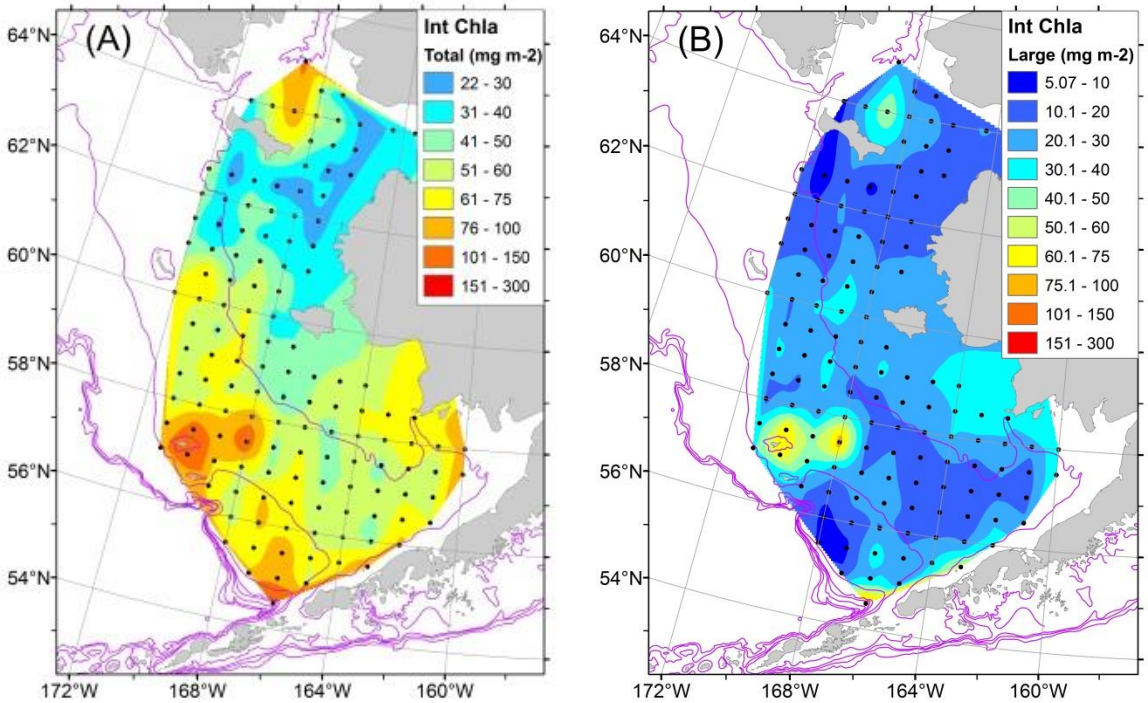
(A)
Int Chla
Total (mg m-2)
22 - 30
31 - 40
41 - 50
51 - 60
61 - 75
76 - 100
101 - 150
151 - 300
64°N
62°N
60°N
58°N
56°N
54°N
172°W
168°W
164°W
160°W
(B)
Int Chla
Large (mg m-2)
5.07 - 10
10.1 - 20
20.1 - 30
30.1 - 40
40.1 - 50
50.1 - 60
60.1 - 75
75.1 - 100
101 - 150
151 - 300
64°N
62°N
60°N
58°N
56°N
54°N
172°W
168°W
164°W
160°W

Figure 2.

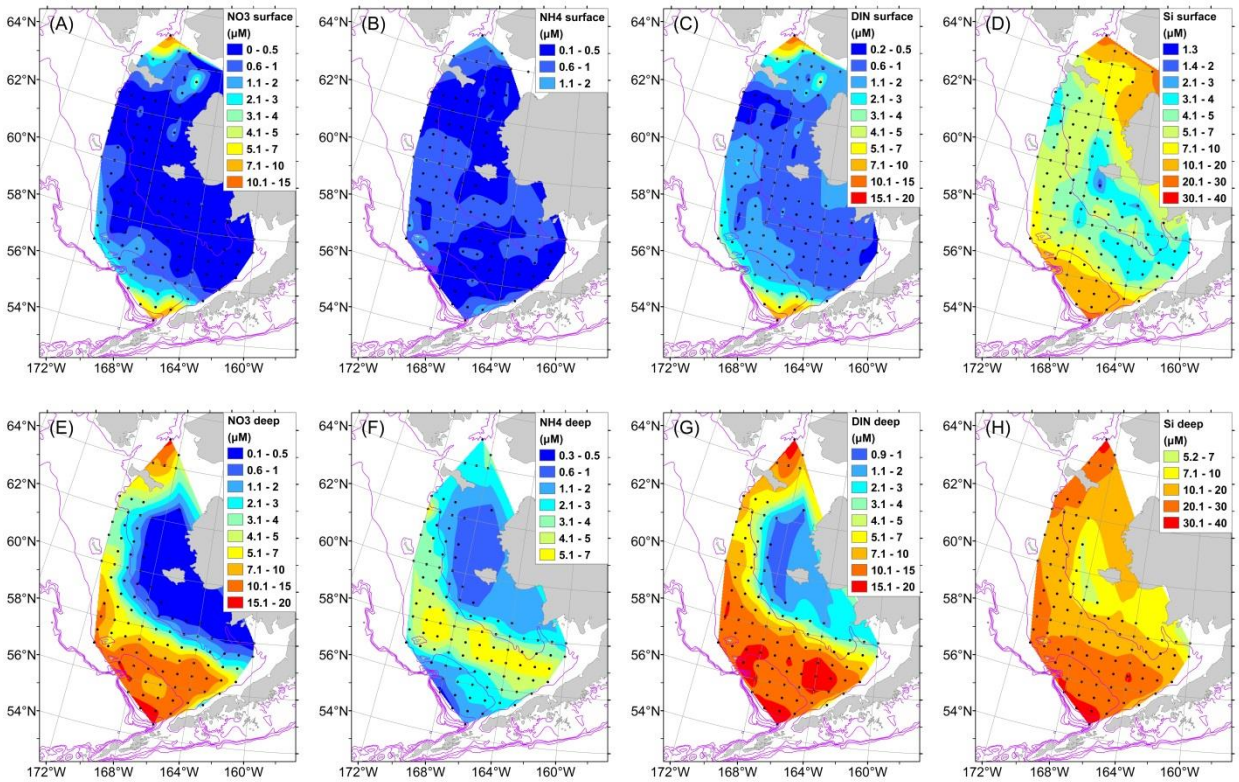
(A)
NO3 surface (µM)
0 - 0.5
0.6 - 1
1.1 - 2
2.1 - 3
3.1 - 4
4.1 - 5
5.1 - 7
7.1 - 10
10.1 - 15
(B)
NH4 surface (µM)
0.1 - 0.5
0.6 - 1
1.1 - 2
(C)
DIN surface (µM)
0.2 - 0.5
0.6 - 1
1.1 - 2
2.1 - 3
3.1 - 4
4.1 - 5
5.1 - 7
7.1 - 10
10.1 - 15
15.1 - 20
(D)
Si surface (µM)
1.3
1.4 - 2
2.1 - 3
3.1 - 4
4.1 - 5
5.1 - 7
7.1 - 10
10.1 - 20
20.1 - 30
30.1 - 40
(E)
NO3 deep (µM)
0.1 - 0.5
0.6 - 1
1.1 - 2
2.1 - 3
3.1 - 4
4.1 - 5
5.1 - 7
7.1 - 10
10.1 - 15
15.1 - 20
(F)
NH4 deep (µM)
0.3 - 0.5
0.6 - 1
1.1 - 2
2.1 - 3
3.1 - 4
4.1 - 5
5.1 - 7
(G)
DIN deep (µM)
0.9 - 1
1.1 - 2
2.1 - 3
3.1 - 4
4.1 - 5
5.1 - 7
7.1 - 10
10.1 - 15
15.1 - 20
(H)
Si deep (µM)
5.2 - 7
7.1 - 10
10.1 - 20
20.1 - 30
30.1 - 40
64°N
62°N
60°N
58°N
56°N
54°N
172°W
168°W
164°W
160°W

Figure 3.

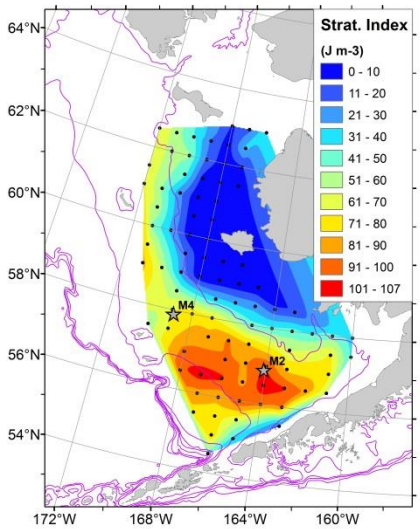
Strat. Index
(J m-3)
0 - 10
11 - 20
21 - 30
31 - 40
41 - 50
51 - 60
61 - 70
71 - 80
81 - 90
91 - 100
101 - 107
64°N
62°N
60°N
58°N
56°N
54°N
172°W
168°W
164°W
160°W
M4
M2

Figure 4.

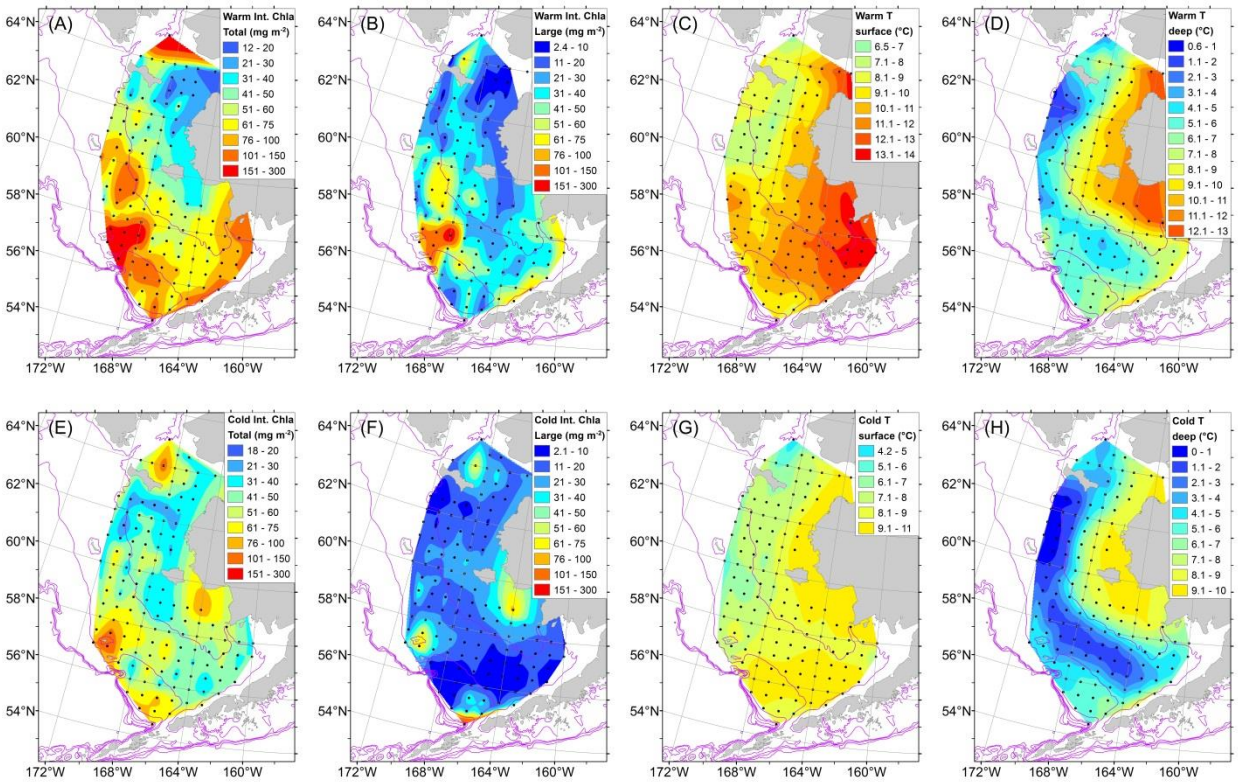
(A)
Warm Int. Chla
Total (mg m-2)
12 - 20
21 - 30
31 - 40
41 - 50
51 - 60
61 - 75
76 - 100
101 - 150
151 - 300
(B)
Warm Int. Chla
Large (mg m-2)
2.4 - 10
11 - 20
21 - 30
31 - 40
41 - 50
51 - 60
61 - 75
76 - 100
101 - 150
151 - 300
(C)
Warm T
surface (°C)
6.5 - 7
7.1 - 8
8.1 - 9
9.1 - 10
10.1 - 11
11.1 - 12
12.1 - 13
13.1 - 14
(D)
Warm T
deep (°C)
0.6 - 1
1.1 - 2
2.1 - 3
3.1 - 4
4.1 - 5
5.1 - 6
6.1 - 7
7.1 - 8
8.1 - 9
9.1 - 10
10.1 - 11
11.1 - 12
12.1 - 13
(E)
Cold Int. Chla
Total (mg m-2)
18 - 20
21 - 30
31 - 40
41 - 50
51 - 60
61 - 75
76 - 100
101 - 150
151 - 300
(F)
Cold Int. Chla
Large (mg m-2)
2.1 - 10
11 - 20
21 - 30
31 - 40
41 - 50
51 - 60
61 - 75
76 - 100
101 - 150
151 - 300
(G)
Cold T
surface (°C)
4.2 - 5
5.1 - 6
6.1 - 7
7.1 - 8
8.1 - 9
9.1 - 11
(H)
Cold T
deep (°C)
0 - 1
1.1 - 2
2.1 - 3
3.1 - 4
4.1 - 5
5.1 - 6
6.1 - 7
7.1 - 8
8.1 - 9
9.1 - 10
64°N
62°N
60°N
58°N
56°N
54°N
172°W
168°W
164°W
160°W

Figure 5.

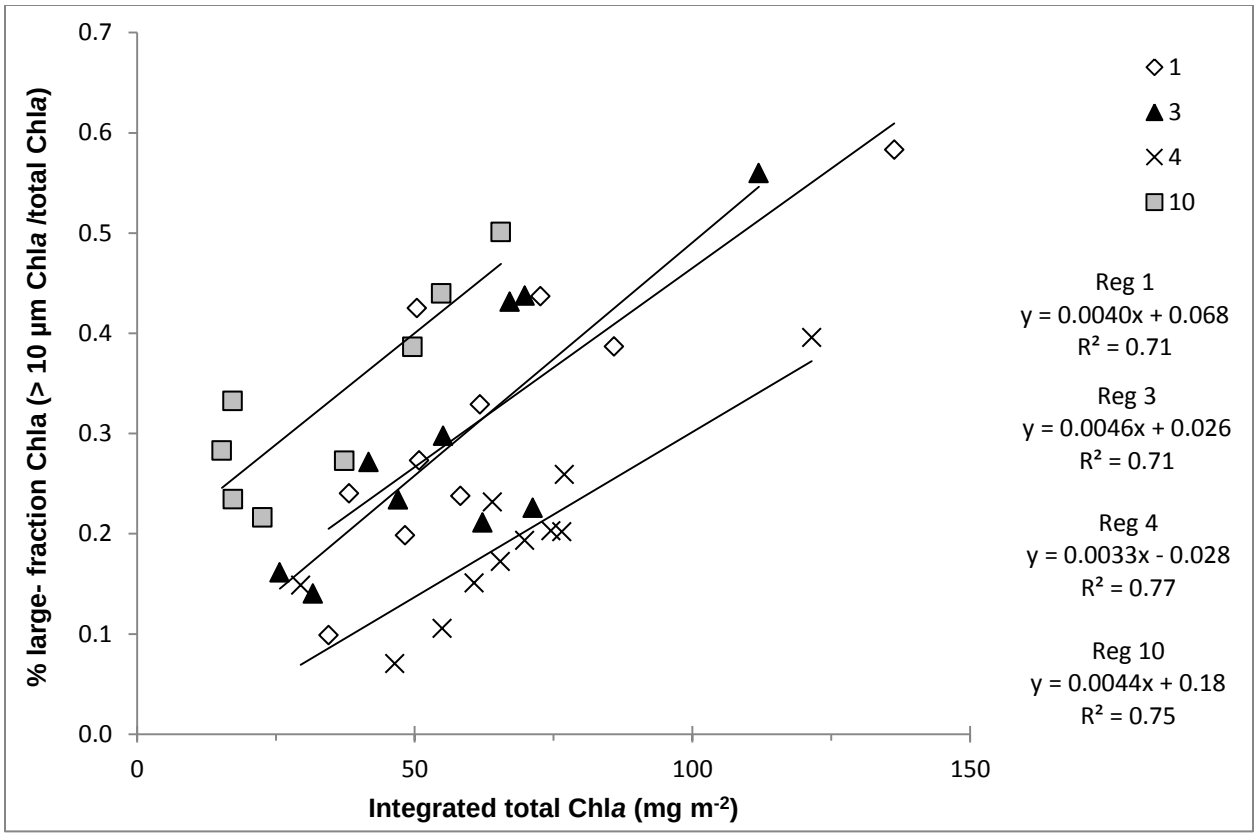
0.7
0.6
0.5
0.4
0.3
0.2
0.1
0.0
0
50
100
150
% large- fraction Chla (> 10 µm Chla /total Chla)
Integrated total Chla (mg m-2)
1
3
4
10
Reg 1
y = 0.0040x + 0.068
R² = 0.71
Reg 3
y = 0.0046x + 0.026
R² = 0.71
Reg 4
y = 0.0033x - 0.028
R² = 0.77
Reg 10
y = 0.0044x + 0.18
R² = 0.75

Figure 6.

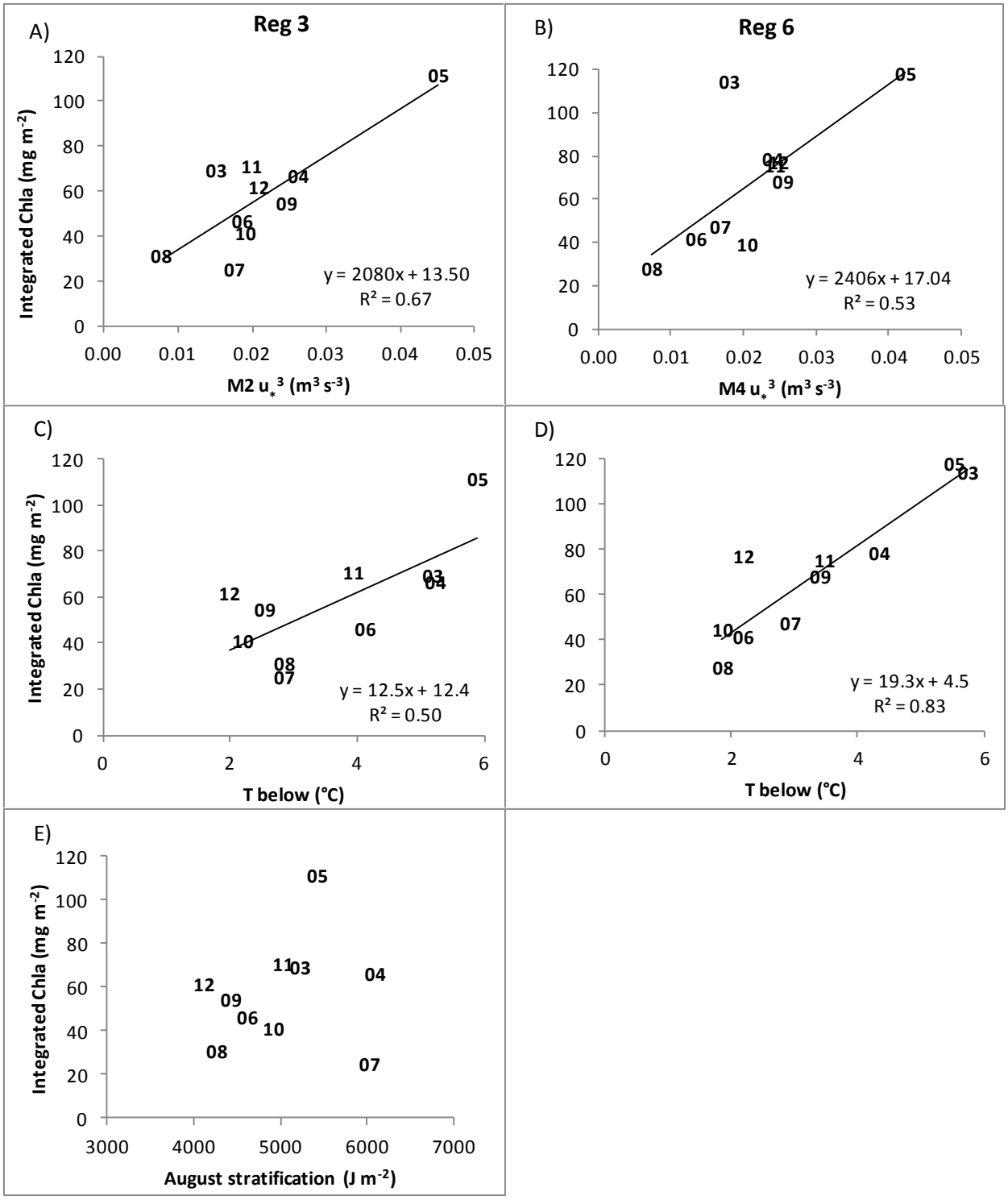
A)
Reg 3
Integrated Chla (mg m-2)
M2 u*3 (m3 s-3)
y = 2080x + 13.50
R² = 0.67
B)
Reg 6
M4 u*3 (m3 s-3)
y = 2406x + 17.04
R² = 0.53
C)
T below (°C)
y = 12.5x + 12.4
R² = 0.50
D)
T below (°C)
y = 19.3x + 4.5
R² = 0.83
E)
August stratification (J m-2)

Figure 7.

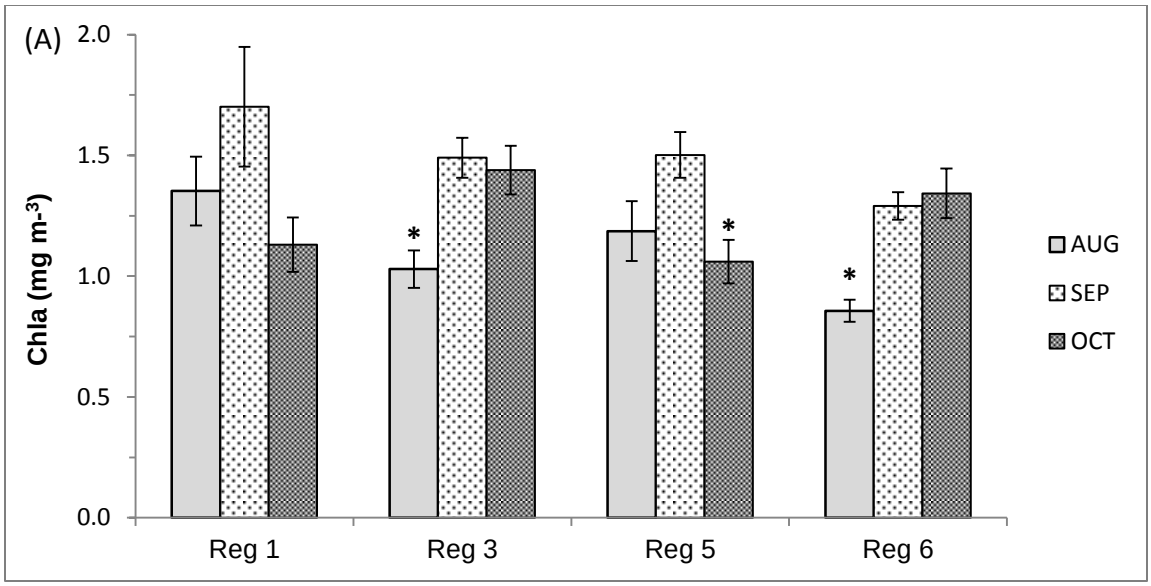
(A)
2.0
1.5
1.0
0.5
0.0
Chla (mg m-3)
*
*
*
Reg 1
Reg 3
Reg 5
Reg 6
AUG
SEP
OCT

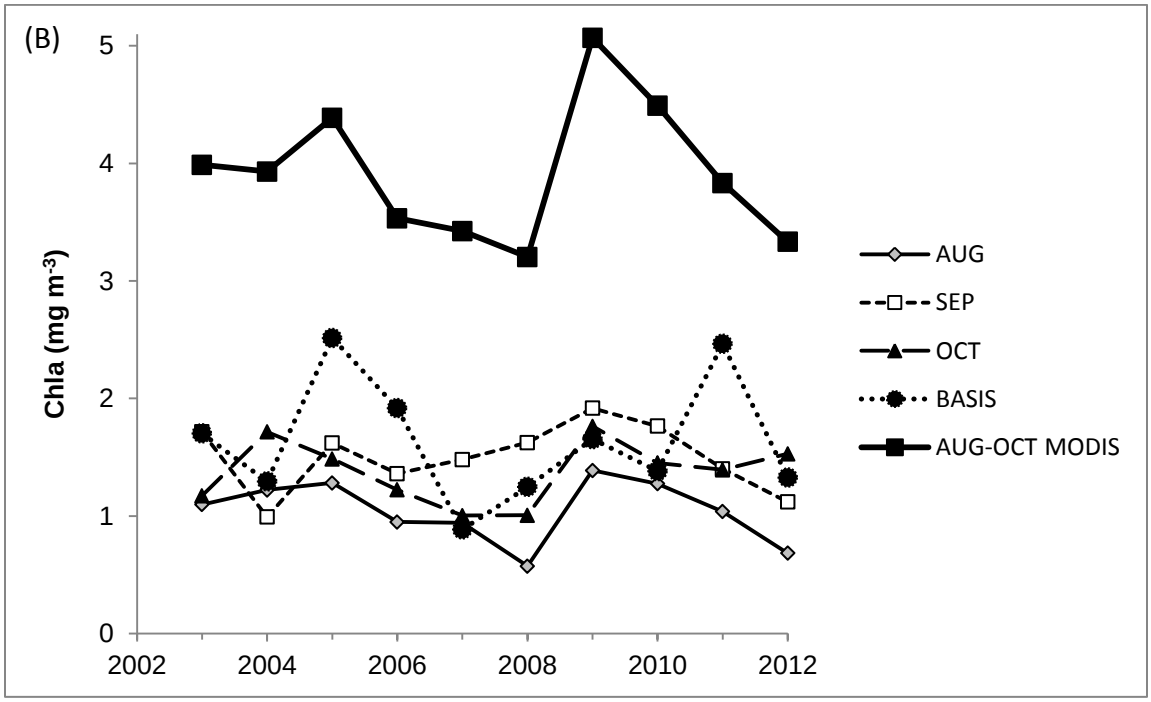
(B)
5
4
3
2
1
0
Chla (mg m-3)
2002
2004
2006
2008
2010
2012
AUG
SEP
OCT
BASIS
AUG-OCT MODIS

Figure 8.

Appendix. Mean values by region and year for surface and deep temperature (T, °C), salinity (S) and nutrients (phosphate, silicic acid, nitrate, ammonium, μM). T and S are means above (surface) and below (deep) the pycnocline. Nutrients are from ~ 5 m (surface) and 30-60 m (deep). Only stations sampled 5 years or more (Fig. 1) were used in the analysis.

T (surface)

| **Region** | 2003 | 2004 | 2005 | 2006 | 2007 | 2008 | 2009 | 2010 | 2011 | 2012 | Grand Avg |
|---|---|---|---|---|---|---|---|---|---|---|---|
| 1 | 11.11 | 10.53 | 11.68 | 10.07 | 10.34 | 9.61 | 9.11 | 8.94 | 9.00 | 9.37 | 10.05 |
| 2 | 11.42 | 12.48 | 12.65 | 9.43 | 10.11 | 8.86 | 9.83 | 8.39 | 8.77 | 7.96 | 10.22 |
| 3 | 11.66 | 12.17 | 11.20 | 9.85 | 10.85 | 8.85 | 7.81 | 8.49 | 8.55 | 8.58 | 9.87 |
| 4 | 10.41 | 10.49 | 10.04 | 10.04 | 10.52 | 9.41 | 8.02 | 9.59 | 8.91 | 8.85 | 9.59 |
| 5 | | 10.57 | 9.74 | 8.91 | 8.02 | | 6.93 | | 8.91 | 6.53 | 8.51 |
| 6 | 9.74 | 11.29 | 8.11 | 9.45 | 7.47 | 7.41 | 7.47 | 7.86 | 7.82 | 6.08 | 8.22 |
| 7 | 9.88 | 11.06 | 8.88 | 8.24 | 9.41 | 7.64 | 8.16 | 7.78 | 7.21 | 7.25 | 8.70 |
| 9 | 7.38 | 8.89 | 6.68 | 7.48 | 6.80 | | 7.50 | 7.11 | 7.36 | 3.84 | 7.15 |
| 10 | | 9.42 | 7.11 | 8.07 | 7.76 | | 7.59 | 7.63 | 6.27 | 5.06 | 7.67 |
| 11 | 7.85 | 9.98 | 7.14 | 7.88 | 8.37 | | 8.25 | 8.47 | 7.65 | 7.17 | 8.13 |
| 12 | 8.67 | 9.07 | | 8.43 | 8.93 | | 6.68 | 5.44 | 5.09 | 6.06 | 7.52 |
| 13 | 7.31 | 10.28 | 7.91 | 7.22 | 8.80 | | 6.92 | 7.54 | 5.91 | 5.04 | 7.34 |
| 14 | 10.52 | 11.98 | 10.28 | 10.41 | 10.37 | | 9.67 | 9.04 | 8.33 | 7.49 | 9.52 |
| 16 | 9.66 | 8.23 | 8.83 | 8.30 | | | | 8.24 | 8.80 | | 8.68 |
| Grand Avg | 10.15 | 10.95 | 9.59 | 8.99 | 9.23 | 8.64 | 8.05 | 8.28 | 7.88 | 7.44 | 8.93 |

T (deep)

| **Region** | 2003 | 2004 | 2005 | 2006 | 2007 | 2008 | 2009 | 2010 | 2011 | 2012 | Grand Avg |
|---|---|---|---|---|---|---|---|---|---|---|---|
| 1 | 7.76 | 7.84 | 7.81 | 7.88 | 5.35 | 6.80 | 7.02 | 5.97 | 6.92 | 5.41 | 6.87 |
| 2 | 9.33 | 9.52 | 9.17 | 7.87 | 6.30 | 6.45 | 7.28 | 7.11 | 6.95 | 6.54 | 7.86 |
| 3 | 5.19 | 5.23 | 5.90 | 4.13 | 2.86 | 2.86 | 2.55 | 2.20 | 3.94 | 1.99 | 3.69 |
| 4 | 6.83 | 6.10 | 6.32 | 5.98 | 5.43 | 4.92 | 5.56 | 5.00 | 5.28 | 5.26 | 5.60 |
| 5 | | 7.58 | 7.46 | 5.54 | 4.16 | | 4.22 | | 4.97 | 3.64 | 5.25 |
| 6 | 5.74 | 4.34 | 5.54 | 2.19 | 2.93 | 1.86 | 3.40 | 1.86 | 3.47 | 2.19 | 3.11 |
| 7 | 9.87 | 9.91 | 8.45 | 7.56 | 7.87 | 6.14 | 7.58 | 7.31 | 7.16 | 6.47 | 7.93 |
| 9 | 6.02 | 3.76 | 3.98 | 1.49 | 0.81 | | 0.71 | 0.72 | 1.86 | 1.05 | 2.21 |
| 10 | | 3.25 | 1.33 | 1.41 | 1.03 | | 1.26 | 1.44 | 0.89 | 4.06 | 1.57 |
| 11 | 7.68 | 9.00 | 6.97 | 6.70 | 7.12 | | 6.41 | 6.12 | 6.83 | 6.34 | 7.01 |
| 12 | 4.42 | 7.01 | | 4.66 | 6.37 | | 3.86 | 5.36 | 3.95 | 5.53 | 5.10 |
| 13 | 5.79 | 6.91 | 7.43 | 4.74 | 6.08 | | 3.70 | 5.52 | 5.10 | 3.22 | 5.21 |
| 14 | 10.17 | 11.41 | 10.16 | 8.12 | 10.26 | | 7.98 | 8.63 | 7.52 | 6.81 | 8.69 |
| 16 | 6.74 | 5.50 | 6.10 | 6.02 | | | | 5.27 | 5.20 | | 5.81 |
| Grand Avg | 7.24 | 6.92 | 6.49 | 5.05 | 4.73 | 4.31 | 4.48 | 4.51 | 4.91 | 4.30 | 5.31 |

S (surface)

| Region | 2003 | 2004 | 2005 | 2006 | 2007 | 2008 | 2009 | 2010 | 2011 | 2012 | Grand Avg |
|---|---|---|---|---|---|---|---|---|---|---|---|
| 1 | 31.57 | 31.67 | 31.81 | 31.74 | 31.79 | 31.75 | 31.81 | 31.68 | 32.02 | 31.84 | 31.76 |
| 2 | 30.92 | 30.89 | 30.58 | 30.55 | 31.09 | 30.76 | 30.56 | 31.08 | 30.59 | 31.05 | 30.82 |
| 3 | 31.63 | 31.70 | 31.74 | 31.43 | 31.37 | 31.49 | 31.44 | 31.32 | 31.45 | 31.41 | 31.49 |
| 4 | 31.86 | 31.88 | 31.96 | 31.92 | 31.94 | 31.63 | 31.95 | 31.81 | 32.09 | 32.08 | 31.95 |
| 5 | | 31.94 | 31.96 | 31.98 | 31.68 | | 31.80 | | 31.71 | 31.68 | 31.81 |
| 6 | 31.93 | 31.86 | 31.98 | 31.49 | 31.52 | 31.43 | 31.43 | 31.16 | 31.33 | 31.37 | 31.50 |
| 7 | 31.25 | 31.21 | 31.12 | 30.85 | 30.95 | 31.12 | 31.18 | 31.22 | 31.05 | 31.03 | 31.08 |
| 9 | 31.45 | 31.56 | 31.78 | 30.99 | 31.06 | | 31.19 | 30.74 | 30.98 | 31.23 | 31.21 |
| 10 | | 31.12 | 31.27 | 30.88 | 31.16 | | 30.95 | 31.11 | 31.06 | 30.58 | 31.07 |
| 11 | 30.54 | 30.31 | 31.02 | 30.56 | 30.63 | | 30.77 | 30.58 | 30.78 | 30.66 | 30.66 |
| 12 | 31.41 | 32.08 | | 31.90 | 31.62 | | 31.47 | 31.63 | 32.00 | 31.72 | 31.74 |
| 13 | 30.55 | 30.82 | 31.21 | 31.31 | 31.45 | | 30.56 | 31.24 | 31.54 | 31.45 | 31.17 |
| 14 | 26.38 | 28.75 | 29.86 | 25.62 | 28.74 | | 27.58 | 28.11 | 28.22 | 28.40 | 27.84 |
| 16 | 32.35 | 32.61 | 32.77 | 32.42 | | | | 32.55 | 32.54 | | 32.54 |
| Grand Avg | 31.02 | 31.20 | 31.38 | 31.00 | 31.21 | 31.31 | 30.94 | 31.04 | 31.16 | 31.20 | 31.14 |

S (deep)

| Region | 2003 | 2004 | 2005 | 2006 | 2007 | 2008 | 2009 | 2010 | 2011 | 2012 | Grand Avg |
|---|---|---|---|---|---|---|---|---|---|---|---|
| 1 | 31.94 | 32.02 | 32.08 | 32.01 | 32.18 | 31.89 | 32.05 | 31.99 | 32.21 | 32.16 | 32.06 |
| 2 | 31.25 | 31.05 | 31.17 | 30.96 | 31.30 | 31.18 | 31.07 | 31.26 | 30.90 | 31.30 | 31.15 |
| 3 | 31.88 | 31.96 | 32.08 | 31.88 | 31.81 | 31.91 | 31.77 | 31.73 | 31.94 | 31.81 | 31.88 |
| 4 | 32.61 | 32.48 | 32.49 | 32.53 | 32.59 | 32.43 | 32.66 | 32.51 | 32.64 | 32.61 | 32.57 |
| 5 | | 32.07 | 32.09 | 32.07 | 31.91 | | 32.24 | | 32.08 | 32.09 | 32.06 |
| 6 | 32.06 | 31.97 | 32.07 | 31.83 | 31.64 | 31.74 | 31.61 | 31.53 | 31.63 | 31.72 | 31.75 |
| 7 | 31.25 | 31.20 | 31.20 | 30.88 | 30.99 | 31.21 | 31.28 | 31.29 | 31.06 | 31.12 | 31.13 |
| 9 | 31.57 | 31.57 | 32.04 | 31.38 | 31.52 | | 31.54 | 31.15 | 31.24 | 31.49 | 31.50 |
| 10 | | 31.13 | 31.60 | 31.37 | 31.75 | | 31.45 | 31.77 | 31.39 | 31.56 | 31.49 |
| 11 | 30.65 | 30.68 | 31.04 | 30.66 | 30.77 | | 30.91 | 30.77 | 30.91 | 30.93 | 30.82 |
| 12 | 31.72 | 32.12 | | 31.99 | 31.80 | | 31.90 | 31.68 | 32.22 | 31.80 | 31.92 |
| 13 | 31.49 | 31.24 | 31.21 | 31.62 | 31.68 | | 31.68 | 31.56 | 31.75 | 32.00 | 31.62 |
| 14 | 27.95 | 29.80 | 29.92 | 29.69 | 29.15 | | 29.98 | 29.80 | 29.51 | 29.71 | 29.51 |
| 16 | 32.74 | 33.09 | 33.22 | 32.74 | | | | 32.91 | 33.02 | | 32.95 |
| Grand Avg | 31.40 | 31.46 | 31.66 | 31.46 | 31.53 | 31.67 | 31.47 | 31.46 | 31.53 | 31.58 | 31.51 |

Phosphate (surface)

| **Region** | 2003 | 2004 | 2005 | 2006 | 2007 | 2008 | 2009 | 2010 | 2011 | 2012 | Grand Avg |
|---|---|---|---|---|---|---|---|---|---|---|---|
| 1 | 0.56 | 0.88 | 0.48 | 0.55 | 0.57 | 0.57 | 0.70 | 0.53 | 0.57 | 0.34 | 0.56 |
| 2 | 0.54 | 0.58 | 0.44 | 0.31 | 0.50 | 0.54 | 0.45 | 0.54 | 0.40 | 0.47 | 0.48 |
| 3 | 0.23 | 0.34 | 0.43 | 0.31 | 0.38 | 0.41 | 0.50 | 0.37 | 0.57 | 0.32 | 0.38 |
| 4 | 0.60 | 0.65 | 0.72 | 0.42 | 0.39 | 0.32 | 0.74 | 0.46 | 0.64 | 0.55 | 0.57 |
| 5 | | 0.43 | 0.52 | 0.59 | 0.56 | | 0.47 | | 0.45 | 0.73 | 0.54 |
| 6 | 0.32 | 0.31 | 0.66 | 0.39 | 0.64 | 0.50 | 0.46 | 0.50 | 0.58 | 0.69 | 0.51 |
| 7 | 0.55 | 0.46 | 0.51 | 0.37 | 0.47 | 0.58 | 0.62 | 0.69 | 0.09 | 0.67 | 0.50 |
| 9 | 0.60 | 0.45 | 0.79 | 0.59 | 0.52 | | 0.39 | 0.70 | 0.72 | 0.92 | 0.62 |
| 10 | | 0.56 | 0.63 | 0.61 | 0.66 | | 0.48 | 0.72 | 0.82 | 0.67 | 0.63 |
| 11 | 0.82 | 0.77 | 0.78 | 0.65 | 0.68 | | 0.54 | 0.77 | 0.45 | 0.62 | 0.67 |
| 12 | 0.48 | 0.22 | | 0.34 | 0.41 | | 0.38 | 0.78 | 1.13 | 0.16 | 0.50 |
| 13 | 0.61 | 0.63 | 0.80 | 0.54 | 0.57 | | 0.54 | 0.84 | 1.13 | 0.64 | 0.71 |
| 14 | 0.64 | 0.57 | 0.96 | 0.53 | 0.99 | | 0.60 | 0.73 | 0.78 | 0.55 | 0.68 |
| 16 | 0.94 | 1.49 | 1.39 | 1.14 | | | | 0.74 | 0.66 | | 1.06 |
| Grand Avg | 0.51 | 0.54 | 0.60 | 0.46 | 0.54 | 0.48 | 0.53 | 0.60 | 0.62 | 0.53 | 0.55 |

Phosphate (deep)

| **Region** | 2003 | 2004 | 2005 | 2006 | 2007 | 2008 | 2009 | 2010 | 2011 | 2012 | Grand Avg |
|---|---|---|---|---|---|---|---|---|---|---|---|
| 1 | 1.51 | 1.23 | 1.40 | 1.34 | 1.64 | 1.24 | 1.14 | 1.06 | 1.18 | 1.21 | 1.29 |
| 2 | 1.23 | 0.91 | 1.09 | 0.58 | 0.83 | 0.81 | 0.93 | 0.83 | 0.78 | 0.61 | 0.84 |
| 3 | 1.54 | 1.54 | 1.49 | 1.39 | 1.67 | 1.36 | 1.46 | 1.33 | 1.45 | 1.38 | 1.45 |
| 4 | 1.37 | 1.25 | 1.46 | 1.19 | 1.57 | 1.47 | 1.32 | 1.30 | 1.18 | 1.19 | 1.29 |
| 5 | | 1.28 | 1.25 | 1.21 | 1.30 | | 1.16 | | 1.44 | 1.40 | 1.30 |
| 6 | | 1.49 | 1.39 | 1.40 | 1.33 | 1.23 | 1.24 | 1.26 | 1.40 | 1.38 | 1.36 |
| 7 | | 0.65 | 0.70 | 0.78 | | 0.85 | 0.55 | 0.83 | 0.18 | 0.87 | 0.74 |
| 9 | 1.16 | 1.09 | 1.58 | 1.22 | 1.66 | | 1.26 | 1.30 | 1.36 | 1.36 | 1.32 |
| 10 | | 1.15 | 1.31 | 1.11 | | | 1.19 | 1.43 | 1.57 | | 1.30 |
| 11 | 1.07 | 0.81 | 0.93 | 0.86 | | | 0.92 | 1.06 | 0.85 | 0.83 | 0.92 |
| 12 | | 0.90 | | | 0.94 | | 1.00 | | 1.82 | | 1.17 |
| 13 | 2.13 | | | 1.06 | 1.32 | | 1.34 | 1.92 | 1.56 | 1.46 | 1.48 |
| 14 | | | | | | | | | | | |
| 16 | 1.47 | 1.86 | 1.81 | 1.51 | | | | 0.91 | | | 1.51 |
| Grand Avg | 1.43 | 1.22 | 1.34 | 1.23 | 1.43 | 1.19 | 1.21 | 1.18 | 1.29 | 1.18 | 1.25 |

Silicic acid (surface)

| Region | 2003 | 2004 | 2005 | 2006 | 2007 | 2008 | 2009 | 2010 | 2011 | 2012 | Grand Avg |
|---|---|---|---|---|---|---|---|---|---|---|---|
| 1 | 9.93 | 15.44 | 7.91 | 12.83 | 6.42 | 12.99 | 9.41 | 8.16 | 12.14 | 3.68 | 9.58 |
| 2 | 3.53 | 6.56 | 1.48 | 2.60 | 1.78 | 7.44 | 2.98 | 6.71 | 3.76 | 6.27 | 4.22 |
| 3 | 2.71 | 6.32 | 5.69 | 3.71 | 1.61 | 5.33 | 5.95 | 3.70 | 9.94 | 3.58 | 4.82 |
| 4 | 14.62 | 17.79 | 13.90 | 10.84 | 10.89 | 10.84 | 10.00 | 7.97 | 17.14 | 13.98 | 12.89 |
| 5 | | 5.83 | 13.23 | 6.22 | 9.43 | | 6.52 | | 2.80 | 9.40 | 7.42 |
| 6 | 3.38 | 5.48 | 5.57 | 2.81 | 8.25 | 6.39 | 5.06 | 5.05 | 5.52 | 6.04 | 5.37 |
| 7 | 2.31 | 3.31 | 3.01 | 2.10 | 1.86 | 7.17 | 5.13 | 7.48 | 1.00 | 9.03 | 4.16 |
| 9 | 5.62 | 5.45 | 8.50 | 2.75 | 5.06 | | 4.56 | 5.49 | 5.12 | 11.58 | 5.75 |
| 10 | | 3.89 | 2.82 | 2.50 | 3.33 | | 3.92 | 5.96 | 10.93 | 11.37 | 4.61 |
| 11 | 8.89 | 5.74 | 4.86 | 4.73 | 3.22 | | 6.72 | 7.15 | 5.36 | 7.61 | 5.93 |
| 12 | 1.07 | 3.54 | | 1.90 | 7.52 | | 4.42 | 11.27 | 23.40 | 1.03 | 7.24 |
| 13 | 8.17 | 7.45 | 4.35 | 5.66 | 9.02 | | 7.41 | 11.84 | 21.07 | 10.77 | 10.20 |
| 14 | 17.92 | 14.51 | 6.84 | 11.21 | 11.70 | | 14.71 | 16.67 | 17.58 | 14.07 | 14.79 |
| 16 | 8.00 | 40.84 | 36.53 | 33.32 | | | | 9.93 | 13.20 | | 23.64 |
| Grand Avg | 6.25 | 7.52 | 5.89 | 5.01 | 4.99 | 7.04 | 6.51 | 7.11 | 9.95 | 7.46 | 6.79 |

Silicic acid (deep)

| Region | 2003 | 2004 | 2005 | 2006 | 2007 | 2008 | 2009 | 2010 | 2011 | 2012 | Grand Avg |
|---|---|---|---|---|---|---|---|---|---|---|---|
| 1 | 29.09 | 18.96 | 25.92 | 32.50 | 29.93 | 20.22 | 17.14 | 18.20 | 23.66 | 20.08 | 23.45 |
| 2 | 16.77 | 12.41 | 10.98 | 7.37 | 7.79 | 11.89 | 11.65 | 14.33 | 9.69 | 8.05 | 11.33 |
| 3 | 23.47 | 24.50 | 21.88 | 22.36 | 23.80 | 20.71 | 18.57 | 17.04 | 27.88 | 20.53 | 22.24 |
| 4 | 25.03 | 24.46 | 28.79 | 27.07 | 26.24 | 30.82 | 22.95 | 22.32 | 24.62 | 25.53 | 25.40 |
| 5 | | 19.97 | 26.86 | 17.63 | 19.50 | | 19.05 | | 25.10 | 24.97 | 21.83 |
| 6 | | 21.29 | 15.84 | 17.08 | 13.21 | 15.95 | 15.09 | 17.36 | 19.52 | 20.50 | 17.87 |
| 7 | | 7.10 | 5.95 | 5.19 | | 12.92 | 4.68 | 10.42 | 1.90 | 11.85 | 8.30 |
| 9 | 17.17 | 13.94 | 23.10 | 8.58 | 21.80 | | 12.27 | 20.50 | 20.03 | 22.32 | 17.62 |
| 10 | | 17.41 | 15.80 | 11.06 | | | 15.48 | 27.30 | 27.73 | | 19.33 |
| 11 | 16.78 | 9.81 | 10.30 | 7.48 | | | 10.14 | 10.31 | 9.98 | 10.53 | 10.24 |
| 12 | | 16.17 | | | 15.51 | | 8.40 | | 39.30 | | 19.84 |
| 13 | 37.71 | | | 13.07 | 24.70 | | 24.97 | 33.25 | 33.08 | 20.43 | 26.25 |
| 14 | | | | | | | | | | | |
| 16 | 25.25 | 49.18 | 44.58 | 39.74 | | | | 14.21 | | | 34.59 |
| Grand Avg | 23.73 | 18.62 | 20.09 | 18.11 | 21.04 | 18.03 | 15.79 | 17.92 | 22.57 | 18.33 | 19.22 |

Nitrate (surface)

| **Region** | 2003 | 2004 | 2005 | 2006 | 2007 | 2008 | 2009 | 2010 | 2011 | 2012 | Grand Avg |
|---|---|---|---|---|---|---|---|---|---|---|---|
| 1 | 1.72 | 4.15 | 2.09 | 1.30 | 3.30 | 0.77 | 3.28 | 1.35 | 1.73 | 0.66 | 1.99 |
| 2 | 0.04 | 0.11 | 0.09 | 0.01 | 0.56 | 0.14 | 0.06 | 0.19 | 0.14 | 0.08 | 0.14 |
| 3 | 0.06 | 0.28 | 0.73 | 0.13 | 0.75 | 0.14 | 0.79 | 0.11 | 1.98 | 0.16 | 0.52 |
| 4 | 1.68 | 3.20 | 3.24 | 0.78 | 0.95 | 0.05 | 4.21 | 0.57 | 3.25 | 2.91 | 2.29 |
| 5 | | 0.08 | 0.87 | 0.90 | 1.75 | | 1.16 | | 0.17 | 4.20 | 1.24 |
| 6 | 0.22 | 0.05 | 1.19 | 0.02 | 1.86 | 0.14 | 0.34 | 0.12 | 0.50 | 0.87 | 0.55 |
| 7 | 0.06 | 0.08 | 0.30 | 0.03 | 0.45 | 0.01 | 0.09 | 0.28 | 0.18 | 0.24 | 0.20 |
| 9 | 0.17 | 0.24 | 2.48 | 0.29 | 0.68 | | 0.08 | 0.12 | 0.17 | 1.22 | 0.59 |
| 10 | | 0.22 | 0.10 | 0.01 | 0.07 | | 0.13 | 0.07 | 0.84 | 0.29 | 0.18 |
| 11 | 0.11 | 0.21 | 0.60 | 0.10 | 0.17 | | 0.71 | 0.08 | 0.09 | 0.11 | 0.25 |
| 12 | 0.25 | 0.16 | | 0.02 | 0.62 | | 1.38 | 3.86 | 9.05 | 0.00 | 2.06 |
| 13 | 0.20 | 0.20 | 0.11 | 0.53 | 0.53 | | 2.30 | 3.02 | 5.01 | 2.72 | 1.89 |
| 14 | 0.35 | 0.12 | 0.08 | 9.12 | 0.34 | | 0.14 | 0.11 | 0.43 | 0.07 | 1.10 |
| 16 | 4.34 | 15.02 | 14.00 | 9.89 | | | | 3.32 | 5.40 | | 8.66 |
| Grand Avg | 0.42 | 0.71 | 1.07 | 0.65 | 0.84 | 0.18 | 1.04 | 0.51 | 1.54 | 0.81 | 0.83 |

Nitrate (deep)

| **Region** | 2003 | 2004 | 2005 | 2006 | 2007 | 2008 | 2009 | 2010 | 2011 | 2012 | Grand Avg |
|---|---|---|---|---|---|---|---|---|---|---|---|
| 1 | 14.09 | 7.18 | 10.27 | 10.87 | 14.83 | 4.88 | 7.51 | 5.36 | 8.91 | 7.91 | 9.27 |
| 2 | 2.03 | 0.78 | 1.42 | 0.35 | 0.90 | 0.49 | 1.76 | 1.08 | 0.90 | 0.23 | 0.87 |
| 3 | 8.45 | 8.73 | 9.12 | 10.86 | 11.81 | 7.27 | 9.08 | 5.99 | 9.61 | 8.41 | 8.86 |
| 4 | 11.98 | 10.31 | 14.70 | 9.83 | 15.75 | 12.36 | 12.49 | 9.75 | 11.18 | 9.85 | 11.38 |
| 5 | | 6.48 | 6.47 | 7.66 | 7.85 | | 7.65 | | 8.70 | 12.35 | 8.18 |
| 6 | | 4.07 | 4.71 | 9.63 | 5.21 | 3.41 | 4.71 | 4.81 | 6.71 | 5.27 | 5.83 |
| 7 | | 0.30 | 0.86 | 1.19 | | 0.32 | 0.10 | 0.58 | 0.10 | 0.95 | 0.62 |
| 9 | 1.17 | 0.98 | 6.45 | 3.64 | 7.55 | | 3.95 | 3.52 | 5.08 | 4.62 | 4.01 |
| 10 | | 1.06 | 2.83 | 1.82 | | | 1.86 | 3.11 | 7.92 | | 3.14 |
| 11 | 0.25 | 0.39 | 1.81 | 0.67 | | | 0.36 | 1.25 | 0.63 | 0.47 | 0.77 |
| 12 | | 4.15 | | | 3.92 | | 7.00 | | 15.80 | | 7.72 |
| 13 | 18.42 | | | 4.96 | 6.15 | | 6.73 | 13.77 | 11.81 | 10.95 | 9.69 |
| 14 | | | | | | | | | | | |
| 16 | 11.45 | 22.02 | 21.37 | 16.13 | | | | 4.56 | | | 15.11 |
| Grand Avg | 8.63 | 4.79 | 7.32 | 7.53 | 8.91 | 4.78 | 5.43 | 4.33 | 7.47 | 6.06 | 6.32 |

Ammonium (surface)

| Region | 2003 | 2004 | 2005 | 2006 | 2007 | 2008 | 2009 | 2010 | 2011 | 2012 | Grand Avg |
|---|---|---|---|---|---|---|---|---|---|---|---|
| 1 | 0.20 | 1.02 | 0.23 | 0.76 | 0.74 | 0.80 | 1.01 | 0.79 | 0.77 | 0.50 | 0.64 |
| 2 | 0.11 | 0.50 | 0.35 | 0.38 | 0.85 | 0.98 | 0.16 | 0.52 | 1.42 | 0.58 | 0.55 |
| 3 | 0.13 | 0.25 | 0.52 | 0.32 | 0.63 | 0.50 | 0.75 | 0.37 | 0.82 | 0.18 | 0.43 |
| 4 | 0.04 | 0.48 | 0.31 | 0.20 | 0.58 | 1.07 | 0.68 | 0.44 | 0.56 | 0.11 | 0.41 |
| 5 | | 0.20 | 1.10 | 1.18 | 1.09 | | 0.47 | | 0.26 | 0.90 | 0.81 |
| 6 | 0.34 | 0.26 | 2.06 | 0.22 | 1.30 | 0.63 | 0.37 | 0.77 | 0.47 | 0.82 | 0.69 |
| 7 | 0.17 | 0.30 | 0.89 | 0.22 | 0.96 | 0.53 | 0.36 | 1.34 | 0.08 | 0.22 | 0.57 |
| 9 | 1.45 | 0.26 | 1.89 | 0.71 | 0.78 | | 0.13 | 0.34 | 0.24 | 1.49 | 0.75 |
| 10 | | 0.08 | 0.42 | 0.08 | 0.27 | | 0.23 | 0.33 | 0.26 | 0.31 | 0.23 |
| 11 | 0.45 | 0.09 | 1.42 | 0.56 | 0.70 | | 0.14 | 0.25 | 0.25 | 0.32 | 0.46 |
| 12 | 0.00 | 1.75 | | 0.30 | 1.17 | | 0.35 | 0.79 | 1.65 | 0.09 | 0.85 |
| 13 | 0.19 | 0.19 | 0.35 | 0.19 | 0.41 | | 0.17 | 0.61 | 1.76 | 0.53 | 0.54 |
| 14 | 0.08 | 0.04 | 1.06 | 0.31 | 3.23 | | 0.60 | 0.59 | 1.18 | 0.26 | 0.77 |
| 16 | 0.81 | 0.95 | 0.42 | 0.27 | | | | 1.76 | 0.45 | | 0.78 |
| Grand Avg | 0.26 | 0.33 | 0.76 | 0.36 | 0.83 | 0.68 | 0.37 | 0.54 | 0.74 | 0.42 | 0.53 |

Ammonium (deep)

| Region | 2003 | 2004 | 2005 | 2006 | 2007 | 2008 | 2009 | 2010 | 2011 | 2012 | Grand Avg |
|---|---|---|---|---|---|---|---|---|---|---|---|
| 1 | 1.27 | 2.63 | 4.69 | 3.97 | 1.72 | 4.38 | 2.97 | 2.99 | 2.67 | 3.66 | 3.06 |
| 2 | 4.41 | 2.89 | 5.79 | 2.81 | 2.19 | 3.57 | 4.67 | 2.55 | 3.37 | 1.76 | 3.15 |
| 3 | 4.59 | 4.15 | 5.67 | 3.98 | 5.51 | 4.00 | 3.64 | 4.52 | 4.58 | 3.27 | 4.29 |
| 4 | 1.54 | 1.25 | 0.79 | 2.86 | 1.76 | 3.10 | 1.40 | 2.41 | 1.00 | 1.64 | 1.65 |
| 5 | | 3.17 | 4.92 | 4.35 | 4.43 | | 0.88 | | 4.98 | 2.41 | 3.95 |
| 6 | | 5.75 | 6.43 | 4.16 | 5.65 | 5.06 | 3.57 | 3.85 | 4.26 | 4.49 | 4.64 |
| 7 | | 1.38 | 2.18 | 2.07 | | 2.44 | 0.44 | 2.16 | 0.20 | 0.25 | 1.50 |
| 9 | 3.02 | 3.23 | 6.47 | 4.05 | 4.48 | | 2.40 | 1.94 | 1.35 | 3.74 | 3.36 |
| 10 | | 1.46 | 4.07 | 4.23 | | | 2.02 | 2.78 | 2.28 | | 2.70 |
| 11 | 0.81 | 0.89 | 3.06 | 1.57 | | | 0.85 | 1.31 | 0.69 | 0.67 | 1.17 |
| 12 | | 0.84 | | | 1.94 | | 0.64 | | 4.33 | | 1.94 |
| 13 | 4.27 | | | 2.35 | 3.25 | | 3.38 | 2.27 | 3.36 | 2.53 | 3.03 |
| 14 | | | | | | | | | | | |
| 16 | 2.90 | 0.22 | 0.50 | 1.36 | | | | 3.02 | | | 1.60 |
| Grand Avg | 3.02 | 2.96 | 4.49 | 3.61 | 3.90 | 3.92 | 2.64 | 2.83 | 3.02 | 2.73 | 3.24 |